DOI: 10.1002/ejoc.201201235

Synthetic Progress in cMyc-Max Oncoprotein Miniaturization: Semi-Online Monitoring Gives Solid-Phase Access to Hydrophobic b(-HLH-)ZIP Peptidosteroid Tweezers

Dieter Verzele[a] and Annemieke Madder*[a]

Dedicated to Professor Dr. Pierre J. De Clercq on the occasion of his 65th birthday

Keywords: Solid-phase synthesis / Peptides / Peptidosteroids / Bioorganic chemistry / Protein models / Leucine zippers

Miniature versions of basic leucine zipper (bZIP) and basic helix–loop–helix zipper (b-HLH-ZIP) transcription factors are promising tools for molecular dissection of the genetic information in a post-genomic context. Despite the opportunities of genome interfering agents based on certain oncogenic zipper proteins, structural mimicry of transcription factors is a delicate undertaking, and experimental fine-tuning through bottom-up organic chemistry could benefit from solid-phase/library approaches. Involved in a variety of human pathologies, we became interested in the miniaturization of the cMyc-Max b-HLH-ZIP oncoprotein, and herein elaborate on our synthetic progress in that direction. A bile acid scaffold was successfully employed as artificial dimerization interface in this new type of transcription factor model. Orthogonality of the applied Alloc/Boc/Fmoc chemistries allowed the synthesis of both homo- and heterodimeric peptidosteroid conjugates, covalently restricted with defined geometrical properties. Recognition peptides were assembled through standard Fmoc/*t*Bu solid-phase peptide synthesis (SPPS) chemistry, assisted by automated procedures for consecutive chain elongation on solid support. Invaluable to monitor present strategy, a photocleavable linker allowed rapid, yet detailed analysis of side chain protected peptide intermediates, liberated from the sampled resin, by reverse-phase HPLC and MALDI-TOF-MS. By decorating each scaffold position with two basic region peptides in a 2×2 design, a first generation of unprecedented b(-HLH-)ZIP peptidosteroids was efficiently obtained. As such, a versatile methodology amenable to library generation is presented.

Introduction

Aberrant modulation of gene expression at the transcriptional level is at the origin of numerous diseases. By dysregulating cell growth and triggering cell proliferation, various oncoproteins carry out their biological functions as transcription factors (TFs),[1] critically relying on their DNA-binding capacities. Directly involved in human tumorigenesis and cancer, the pivotal Myc member[2] of the surrounding Myc/Max/Mad network[3] is a prominent example of how these proteins are promising targets towards novel chemotherapeutics.[4,5] The deregulated proliferation of Myc by overexpression has been implicated in the progression of many aggressive malignancies, including Burkitt's lymphoma, neuroblastomas, and small-cell lung cancers.

Although sharing a similar mode of binding DNA target sites with the scrutinized basic leucine zipper (bZIP) equivalents, artificial mimics of these basic helix–loop–helix zipper (b-HLH-ZIP) TFs are conspicuously few. Despite the exceptional total chemical synthesis (172 residues) yielding a covalently stitched replica of the vertebrate cMyc-Max (proto-)oncoprotein dimer achieved by Kent et al. in 1995 (Figure 1),[6] translation of this precedent towards miniature peptide derivatives is long overdue. A supplementary loop in the replaceable HLH-ZIP dimerization interface being the only salient difference, development of synthetic models of the cMyc and Max proteins carves out a niche for innovative initiatives. The preponderance of leucine zipper designs has been further supplemented by the singular MyoD-MyoD mimic, communicated by Morii et al. before finally resorting to the GCN4 bZIP-standard (vide infra).[7] Despite the lack of a zipper region in the dimerization interface, similarities between the loop-containing b-HLH-ZIP and this b-HLH type of TF[8] offer excellent precedent for the current work.

In spite of the advances in the de novo development of such peptide miniatures, progress in this area has been slow compared to the wealth of available high-resolution data.

[a] Laboratory for Organic and Biomimetic Chemistry, Department of Organic Chemistry, Faculty of Sciences, Ghent University,
Krijgslaan 281 (S4), 9000 Ghent, Belgium
Fax: +32-9-264-4998
E-mail: annemieke.madder@ugent.be
Homepage: www.orgchem.ugent.be
Supporting information for this article is available on the WWW under http://dx.doi.org/10.1002/ejoc.201201235.

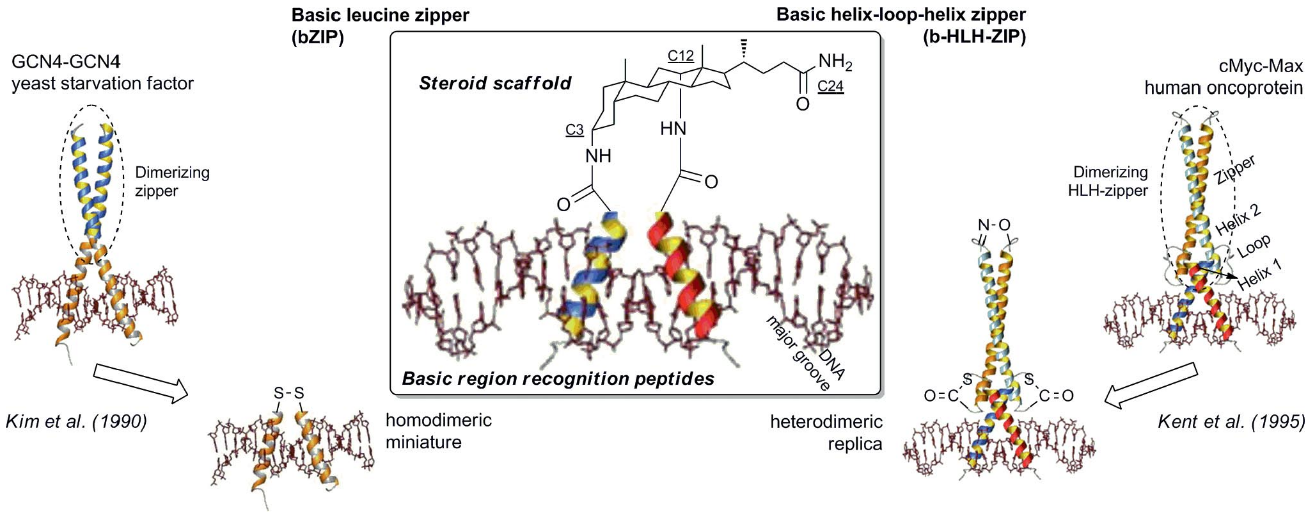

Figure 1. Similar bipartite arrangement of bZIP (left) and b-HLH-ZIP (right) transcription factors, pictorial illustration of the original artificial counterparts by Kim et al. and Kent et al., and our heterodimeric peptidosteroid design (box, not scaled).

Only a handful of bottom-up synthetic approaches have succeeded in mimicking the DNA-recognizing potential of naturally occurring TFs by minimized versions. Deduction of reliable binding principles or recognition rules has been hampered by the large variability of TF folds and discrimination mechanisms. A universal pairing code for the recognition between natural amino acids (AAs) and nucleic acids has yet to be generalized, and only tentative guidelines have been established.[9,10] The fragile balance between structural minimization and biophysical outcome additionally impedes the rational design of downsized mimics and conspires against biomimetic efforts, which demand dedicated trial-and-error tuning of the empirical constraints. Solid-phase/library initiatives are therefore desirable. Remarkably, various b-HLH and b-HLH-ZIP (i.e., loop-containing) proteins display only limited DNA affinity and/or specificity outside of living cells, despite their precise physiological regulation in vivo. In this respect, Myc (proto-)oncoproteins are often called “enigmatic”, as they hide their details during many in vitro assays.[11] Given (a) the influence of loop-projecting DNA contacts,[12] (b) the ambiguous role of loop-associated flexibility,[13] (c) the constraining/stabilizing interactions with essential accessory mediators of the transcriptional machinery in vivo,[14] and (d) the particular regulatory subtleness of these proteins, the scarcity of successful literature precedents might hint towards the daunting nature of the corresponding miniaturization attempts.[15,16]

Considering the variety of challenging opportunities, the present work aims to make contributions to this research area by expanding the repertoire of miniature TF models. Besides the simple desire to mimic Nature, such peptide probes hold the potential to assess the implications of the exquisite selectivity of natural TFs on the control of gene expression. An emerging area in the current post-genomic era, we previously highlighted the pharmacological significance of such TF mimics.[17,18] By allowing the unlimited introduction of artificial elements into the peptidic framework, there exists no doubt about the virtues of organic synthesis for these objectives.

The eukaryotic bZIP and b-HLH-ZIP motifs (Figure 1) are among the simplest protein structures able to bind the DNA major groove in a sequence-specific way.[12c,19–21] Relying on the formation of non-covalent dimers, most of the direct contacts between the TF residues and the DNA nucleobases are made within the recognition α-helices of the so-called basic region, which fork across the major groove to grip the double helix in a tweezer-like fashion. The modularity and tractability of the zipper-type proteins has made them attractive frameworks for the development of artificial counterparts. The bipartite arrangement readily suggests design opportunities, as illustrated in Figure 1, and peptides derived from the basic region can serve as the simplest modules to target specific DNA sequences. In this respect, albeit conceptual, such an approach makes the bZIP, b-HLH-ZIP, and b-HLH proteins uniform in terms of design.

Various innovative strategies have been implemented to meet thermodynamic requirements[22] in miniaturization efforts.[23] Given the vital role of dimerization to mediate tight major groove recognition,[24] the extended C-terminal dimerization domain has often been replaced by artificial connectors, both covalent and non-covalent. Showing a rare structural transparency despite the debatable practical relevance, the most progress has by far been made with the classical GCN4 leucine zipper basic region peptide, as mentioned earlier. In conjunction with (total synthesis) endeavors towards larger constructs, and complemented by numerous biotechnological and semisynthetic approaches, several so-called minimalistic strategies have been reported, next to the development of models other than the zipper-type.[25,26] The current contribution exploits the chemical approach, using bottom-up organic synthesis to develop C-terminally dimerized b(-HLH-)ZIP-like models of reduced size, simultaneously targeting the DNA major groove by two peptide strands comprising natural residues. In the seminal 1990 publication of Kim et al., a simple disulfide bridge sufficed for tethering the GCN4 basic region peptides (Figure 1).[27,28] Since then, a substantial number of attempts have been directed towards the incorporation of dedicated surrogate modules with increasing complexity. These include an N^{α}-,N^{ε}-lysine linkage (Ebright et al.),[29] a bis(terpyridyl)iron(II) coordination complex (Schepartz et al.),[30] a β-cyclodextrin:adamantyl host–guest inclusion complex and bridged enantiomeric biphenyl derivatives (Morii et al.),[31] and a photoresponsive azobenzene moiety (Mascareñas et al.).[32]

For the understanding of DNA–protein recognition and the principles of TF mimicry, macro/supramolecular assemblies with specific architectural features and/or physicochemical properties are still needed. While a decade has passed since Mascareñas' homodimeric GCN4-GCN4 phototrigger, the contrasting void of HLH counterparts stimulated initiatives from our own group. We herein report on our methodological progress towards the first generation of downsized b(-HLH-)ZIP models with an emphasis on the therapeutically relevant cMyc-Max oncoprotein.

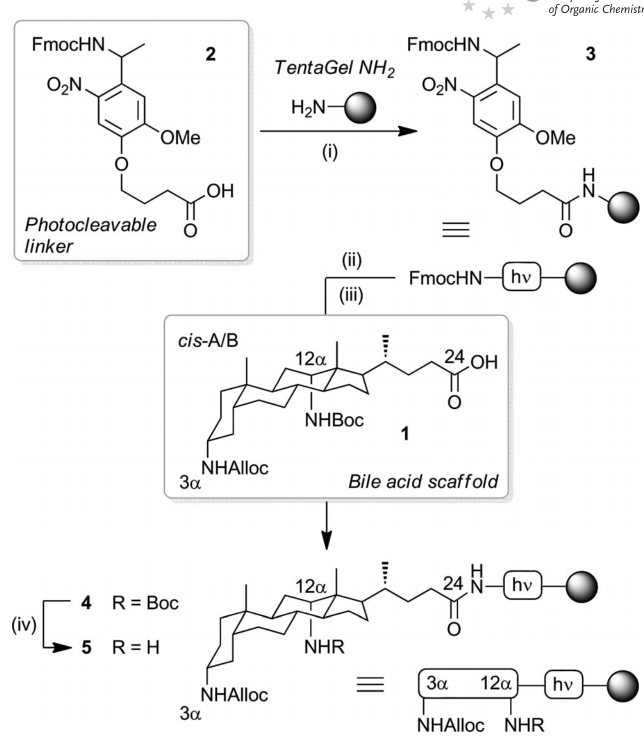

Scheme 1. Preparing for the linear SPPS strategy: Synthesis of solid-supported scaffold starting material **5** through immobilization of steroid scaffold **1** via photolabile linker resin **3**. Reagents and conditions: (i) PyBOP, DIPEA, DMF, r.t., double coupling: 3 + 5 h. (ii) Piperidine in DMF (20% v/v), r.t., triple deprotection: 2 + 5 + 15 min. (iii) (a) Scaffold **1**, PyBOP, DIPEA, DMF, r.t., single coupling overnight; (b) 1-AcIm, $CHCl_3$, r.t., overnight. (iv) TFA in DCM (20% v/v), r.t., triple deprotection: 2 + 5 + 15 min (washing included DIPEA in DMF: 10% v/v).

Results and Discussion

b(-HLH-)ZIP Peptidosteroids: Preparing for a Linear, Monitored SPPS Approach

The present work harnessed a steroid framework as an artificial dimerization interface displaying defined geometrical features (Figure 1 and Scheme 1). Among the variety of molecular scaffolds (templates) used in supramolecular chemistry, steroids in general and bile acids in particular are versatile synthons for applications based on cooperativity and multivalency.[33] The interest in these carbocycles is readily explained by their unique combination of biocompatibility, chirality, high availability, and various functionalization patterns that can be modified in a tunable manner. The well-spaced array of selectively addressable functionalities, distributed around the tetracyclic backbone, and the curved cavity profile resulting from the *cis*-A/B ring junction are ideally suited for receptor design. Pioneered by Still et al.,[34] peptidosteroid libraries and macrocycles are now accessible.[35] Further interest has been cast on the improved pharmacological characteristics of peptides, proteins, and Lipinski structures as drug candidates in a so-called Trojan Horse strategy upon conjugation.[33b–33e,36]

Compared to the large volume of high-resolution data, solved structures of HLH-containing proteins are relatively sparse, and the X-ray views of cMyc-Max and Mad-Max heterodimeric complexes by Burley et al. are a particularly important achievement.[12c] From a structural point of view, the extended dimerization interface of the natural (HLH-)zipper proteins is regarded as a supramolecular scaffold to preorganize, stabilize, and present the relatively small, N-terminal recognition α-helices in an appropriate geometrical positioning relative to the DNA duplex. Because dimerization is a prerequisite, proper docking of the peptides in the DNA major groove is another necessity. Codirectional orientation (so-called α-stereochemistry) and suitable spatial arrangement (ca. 7 Å apart) of the C3–C12 steroid appendages thus offers an attractive starting point to seize the DNA duplex, and thereby, their slight divergence[37] is a further asset. Ligated onto *O*-alkylated cholic acid derivatives in solution, the increased α-helical content of the homotrimeric miniproteins (up to 3 × 37 = 111 AAs) of Wang et al. bears special mentioning in the current b(-HLH-)ZIP story.[38] Mutual induction of α-helicity by the proximal, codirectional peptide strands might thus be anticipated.[39] Next to enhancing stability of the recognition helix, selective binding can be increased upon restriction of the conformational flexibility of the residues that form specific contacts with the nucleobases.[13,14,26] Through a series of homo- and heterodimeric GCN4-based designs, the importance and subtleness of scaffold geometry, rigidity, and chirality was assessed by both the Schepartz and Morii groups.[30,31] Interestingly, the small *cis*-azobenzene unit of the molecular switch[32] designed by Mascareñas et al. shows dimensions and stiffness comparable to our steroid.

A concise route towards dipodal building block **1** (C3α-NHAlloc, C12α-NHBoc-diamino-5β-cholan-24-oic acid; Scheme 1), prepared in just six simple steps from commercially available deoxycholic acid (3α,12α-dihydroxy-5β-cholan-24-oic acid), was developed in our group.[40,41] Basic region peptides have now been constructed at both the C3α and C12α amine groups through stepwise, linear solid-phase peptide synthesis (SPPS).[42,43] The natural spacer and carboxylic acid moiety at the C24 position conveniently enable anchoring of our steroid scaffold to a solid-phase resin. Compatible with a broad range of chemical conditions, the multidimensional protecting group (PG) strategy thereby hinged on the introduction of Holmes' nitroveratryl-based photosensitive linker **2** (4-{4-[1-(9-fluorenylmethoxycarbonylamino)ethyl]-2-methoxy-5-nitrophenoxy}-butanoic acid)[44] to yield supported counterpart **3** immobilized on TentaGel NH_2. With light as a reagent, photolytic cleavage of a chemical bond by the absorption of a photon can only occur through a limited number of pathways, which results in superior orthogonality, and hence, minimization of premature loss and controlled liberation of the attached species at any given time. Fine-tuned through different substituents by Holmes et al.,[45] this *o*-nitrobenzyl-derived linker shows excellent photoreactivity, with release of primary carboxamide species upon irradiation with UV light.[46]

To save on precious scaffold material, a single coupling of a slight excess amount of the substrate was performed overnight. Quantitative resin derivatization was monitored by common color tests[47] by visually detecting resin-bound amino groups with specific reagents. Whereas a simple TNBS (2,4,6-trinitrobenzenesulfonic acid) test allowed the conversion to be followed until construct **4** was obtained, the in-house-developed NF31 test was required to follow reactions at the hindered C12 amino group.[48] Considering the intricacies of the desired b(-HLH-)ZIP peptidosteroids, thorough verification of intermediate compounds is, however, of paramount importance. Therefore, evaluation was complemented by ESI-MS, which was ultimately substituted by MALDI-TOF-MS and reverse-phase (RP)-HPLC analysis upon subsequent decoration. The unique reactivity of the photocleavable handle furnishes a convenient system for advanced monitoring in a semi-online fashion.[49] Samples for detailed analysis are readily available upon simple irradiation of resin aliquots in an appropriate solvent. Only minute quantities are needed for proper evaluation at every stage of the synthesis. The mild cleavage conditions thereby allow the non-destructive release of side chain protected intermediates. Although Moss et al. recently disclosed an optimized procedure for mass spectrometric analysis of protected, synthetic peptides,[50] these compounds remain a challenge for RP-HPLC and mass spectrometry, and the analytical "dos and don'ts" regarding our hydrophobic macromolecules form a vital part of the present contribution.

Aiming for Diversity in a 2 × 2 Dimeric Peptidosteroid Library Setup

From C12 Monomeric Peptidosteroids ...

Relying on the established orthogonality of the C3 NHAlloc and C12 NHBoc scaffold differentiation, functionalization of the C12 position should precede C3 derivatization because of steric constraints. Already suffering from steric impediments of the steroid framework, additional hindrance upon prior C3 derivatization could render the C12 position inaccessible. Acidic NHBoc cleavage prior to peptide generation therefore accommodates the use of standard AAs, which are side chain protected by acid-labile moieties in the Fmoc/*t*Bu SPPS approach. Manual attachment of the very first residue to solid-supported **5** preceded the automated generation of the first basic region peptides at the C12 position of the resin-bound scaffold, and this ensured adequate coupling at the hindered steroid appendage (Scheme 2). A standard PyBOP [benzotriazol-1-yl-*N*-oxy-tris(pyrrolidino)phosphonium hexafluorophosphate] mediated procedure provided straightforward introduction of glutamine and asparagine, which were both side chain protected with a bulky trityl moiety. Consecutive automated chain elongation from the C terminus to the N terminus resulted in side chain protected, monomeric intermediates. After N^{α}-Fmoc deprotection of **6** and **7**, synthesis of the GCN4 peptide at resin **8** and cMyc peptide at **9** yielded peptidosteroids **10** and **11**, respectively. Although the 23-residue GCN4 peptide by Kim et al.[51] has become popular, as minimal sequence is required for sequence-specific binding by α-helix formation, the significantly shorter MyoD mimic of Morii et al., truncated at both the N and C termini, supports the potential of the current cMyc/Max peptide length (only 16 AAs), containing the essential DNA-contacting interface and key residues.

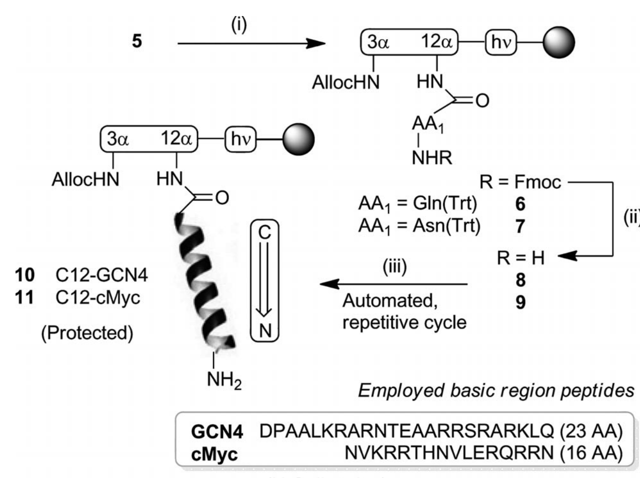

Scheme 2. Synthesis of monomeric C12 peptidosteroid intermediates: manual introduction of initial residue and automated SPPS of the first strand at the C12 steroid position.[52] Reagents and conditions: (i) N^{α}-Fmoc-protected Gln(Trt) or Asn(Trt), PyBOP, DIPEA, DMF, r.t., double coupling: 4 + 4 h. (ii) Piperidine in DMF (20% v/v), r.t., triple deprotection: 2 + 5 + 15 min. (iii) Until completion (with intermediate sampling): (a) N^{α}-Fmoc-protected residue, HBTU, DIPEA, NMP (+ DMF trace), r.t., single coupling: 3 h; (b) piperidine in NMP (40% v/v), r.t., triple deprotection: 2 + 5 + 15 min.

Given that the outcome of an extended linear procedure on the solid phase often depends on minutiae,[43] different parameters of the automated protocol were carefully con-

Table 1. Semi-online monitoring: side chain protected C12 peptidosteroid intermediates cleaved from consecutive resin samples.[a–c]

			AA_1	$AA_2 \rightarrow AA_n$ ($C \rightarrow N$ direction)					No. of AAs
				Sample 1	*Sample 2*	*Sample 3*	*Sample 4*	*Sample 5*	
GCN4	**10**	bZIP	Q (= **8**)	LKRAR	SRRAA	ETNRA	RKLAA	PD	23
cMyc	**11**	b-HLH-ZIP	N (= **9**)	RRQRE	LVNHT	RRKVN	–		16

[a] During automated synthesis and (intermediate) cleavage (i.e., analysis), peptides were protected with standard side chain PGs.[52] Peptidosteroids were released (and analyzed) as C24 carboxamides upon UV-light irradiation of the corresponding resin,[46] which was sampled after Fmoc deprotection of the N terminus. [b] See Figure 2 for RP-HPLC details of the cMyc synthesis. [c] See Supporting Information for further RP-HPLC details of these semi-online monitoring efforts: Table S4 & Figures S9–S11.

sidered, and the integrities of the peptides were monitored at regular sequence intervals. Given that standardized SPPS protocols are inherently restricted to the routine application of a sequential assembly of 50 residues on average, the particular steroid moiety could further impair synthetic viability. Close proximity of the covalently constrained peptides might considerably affect the synthesis, which would prevent reliable derivatization as a result of significant hindrance and/or interstrand interactions. The hydrophobic nature of the carbocyclic framework could result in particular physicochemical features and further complicate both preparation and analysis. Next to the so-called pseudodilution effect of low-loaded resins, solvation and accessibility of the generated peptides might benefit from using NMP (*N*-methylpyrrolidone) as a solvent.[53] Trying to ensure adequate derivatization while obviating double coupling steps, an extended 3-h coupling period was allowed,[54] whereas the concentration of the HBTU {1-[bis(dimethylamino)methylene]-1*H*-benzotriazolium hexafluorophosphate 3-oxide} coupling mixture (0.16 M of active species) was considered the central parameter for reliable generation of the extended sequences.[55] Presented in Table 1, stop commands were incorporated at particular positions of the automated protocol. Sampling after NHFmoc deprotection should enhance compatibility of the side chain protected intermediates with the analytical techniques. The unprotected amino terminus facilitates both elution in reverse-phase chromatography and ionization during mass spectrometry. The essential crystallization during sample preparation for MALDI-TOF-MS might additionally be affected by the presence of the polar N-terminal moiety.

Monitoring of the current protocol by consecutive, photolytically cleaved samples[56] proved efficient and allowed reliable evaluation of the synthetic outcome. Initial MALDI-TOF-MS data confirmed the identity of the desired intermediate and final peptides. Furthermore, excellent results were obtained with RP-HPLC (Figure 2), and analysis of the protected peptide segments relying on chromatography offers a valuable tool for facilitated monitoring and evaluation in cases where MALDI-TOF-MS lacks reliability or fails (see the Supporting Information for further RP-HPLC details of these semi-online monitoring efforts: Table S4 & Figures S9–S11). Whereas side chain PGs allow sensitive UV detection, free N termini assure proper elution of the hydrophobic compounds. However, demonstrating the influence of the steroid moiety, application of a C18/100 Å stationary phase resulted in severe tailing and ultimate failure of analysis, once reaching/exceeding ca. 16 residues,[57] in contrast to non-scaffolded counterparts. This outcome reflects the augmented lypophilicity and/or bulkiness of the peptidosteroid conjugates, and in-

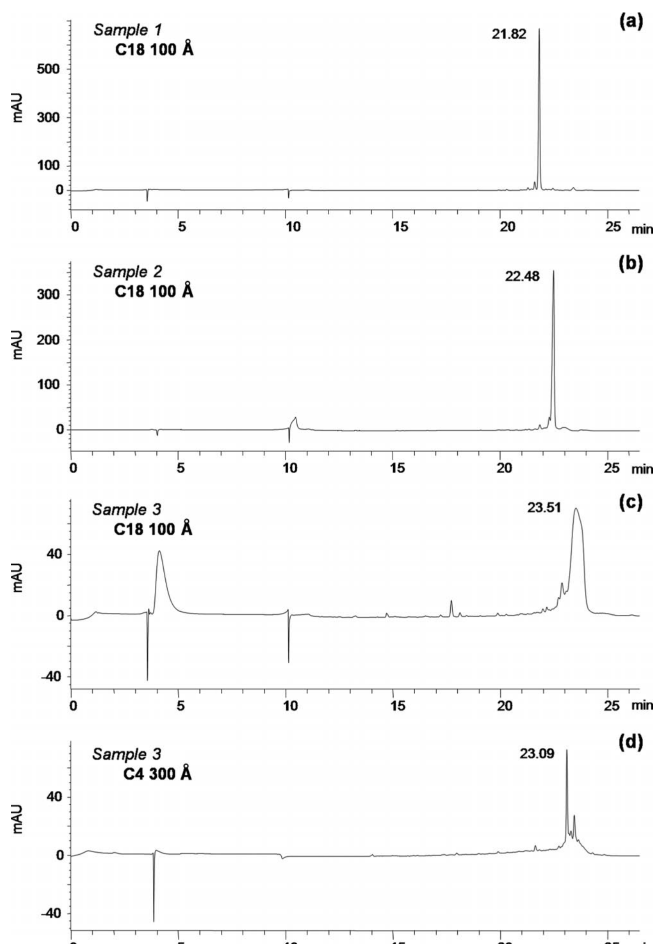

Figure 2. Semi-online monitoring: RP-HPLC (254 nm, gradient 1)[58] of side chain protected C12 peptidosteroid intermediates from the synthesis of cMyc monomer **11** cleaved from consecutive resin samples. See Table 1: (a) *Sample 1*, (b) *Sample 2*, and (c) *Sample 3* (i.e., complete C12 monomer) analyzed with the C18/100 Å column, and (d) *Sample 3* reanalyzed with the C4/300 Å column.

creased stationary phase polarity and/or pore-size seemed necessary. Application of a C4/300 Å stationary phase in that case provided adequate, sharp elution of both **10** and **11**.

... through Key C3 Manipulations ...

bZIP and b-HLH-ZIP proteins have many members that form homo- and heterodimers, a feature that significantly expands the repertoire of DNA-binding specificities from a limited number of protein partners (i.e., combinatorial gene regulation).[24] Although transcription regulation by zipper-type proteins is often mediated by heterodimerization, the majority of synthetic miniature designs has focused on the homodimeric bZIP-GCN4 protein, as covered earlier. As a result of orthogonal N protection, a unique feature of the applied scaffold is the straightforward solid-phase generation of homo- and heterodimeric peptidosteroid tweezers. Steroid conjugation further confers enhanced biostability[59] (next to bioavailability) compared to non-scaffolded peptide counterparts, as mentioned above,[60] and the associated partners are covalently secured. Whereas natural dimerization networks are governed by non-covalent interactions, the present strategy allows a stable connection between both partners, which facilitates further studies. The automated solid-phase approach should be amenable to the parallel synthesis of a b(-HLH-)ZIP library, and this offers the significant advantage to accelerate the meticulous adjustment of recognition capabilities. As the sole literature precedent of such initiatives, the value of a library strategy in TF mimicry was noted in 1996 by Ebright et al., who reported comparable but less-sophisticated bZIP heterodimers with an N^{α}-,N^{ε}-lysine linkage on solid phase.[29] To explore the potential of solid-phase methodology for generating molecular diversity, a 2×2 combination of the GCN4 bZIP and cMyc/Max b-HLH-ZIP monomeric basic region peptides to afford four different, dimeric peptidosteroids (vide infra: Scheme 4) was applied. After parallel C12 decoration of construct **5** with the GCN4 or cMyc sequence, both resins were portioned into two new batches prior to C3 assembly. At the C3 position, once again either the cMyc strand or the related Max strand was synthesized. Structurally, the obtained peptidosteroids consist of either 16 + 16 or 16 + 23 residues, and this represents either homo- or heterodimeric constructs in a quasi- or non-symmetrical arrangement. Whereas the former represent miniature models of natural b-HLH-ZIP combinations, the latter are non-natural conjugates of a yeast bZIP-peptide and a biologically unrelated mammalian b-HLH-ZIP-strand.[61] Both the bZIP + b-HLH-ZIP combinations and the synthetic miniature models of the naturally occurring b-HLH-ZIP Myc-Max network are unprecedented.

Strategically, prior capping of the C12 N terminus is mandatory to proceed towards synthesis of the second strand at the C3 position. Mild overnight treatment of resins **10** and **11** with an excess amount of 1-AcIm (1-acetylimidazole) in $CHCl_3$ provided satisfying acetylation, furnishing **12** and **13**, respectively (Figure 3). Subsequent removal of the C3 NHAlloc PG proceeded smoothly, yet one equivalent of the palladium catalyst was used to improve workability at the µmol scale. In the complex chemical context of the present peptidosteroid intermediates, it was opted to rely on the firmly established procedure of Guibé et al.,[62] which involves palladium-catalyzed hydrostannolysis with tributyltin hydride as the nucleophilic scavenger in the presence of a proton source. To further suppress undesired back-allylation and ensure rapid conversion, a supplementary morpholine scavenger was added in excess amount. Whereas a variety of proton donors has been reported, simple application of *moist* DCM (dichloromethane) provided rapid degradation of the deprotection intermediates. Next to satisfying MALDI-TOF-MS analysis, excellent RP-HPLC results with the C18/100 Å column were obtained (Figure 3). Removal of the lipophilic NHAlloc moiety and/or liberation of the hydrophilic C3 amino group appreciably influenced chromatographic behavior, compared to the precluded C18/100 Å elution of both **10** and **11** (and capped counterparts **12** and **13**).

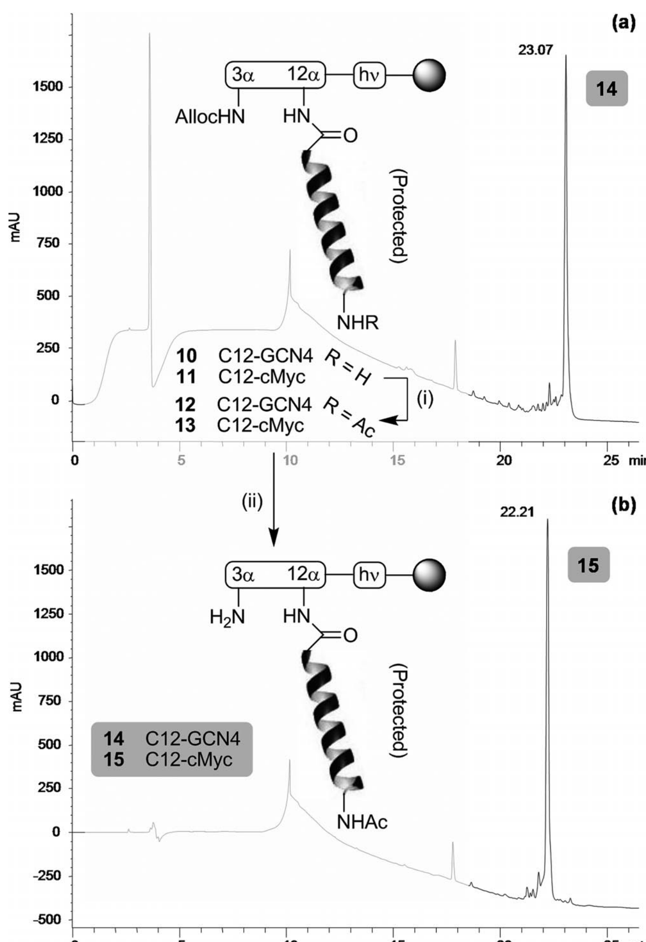

Figure 3. From C12 monomers to C3–C12 dimers through N-terminal acetylation and key C3 NHAlloc removal: RP-HPLC (C18/100 Å, 214 nm, gradient 1)[58] of (a) GCN4-appended **14** and (b) cMyc-appended **15**. Reagents and conditions: (i) 1-AcIm, $CHCl_3$, r.t., overnight. (ii) $Pd(PPh_3)_4$, Bu_3SnH, morpholine, DCM, r.t., single deprotection: 2 h.

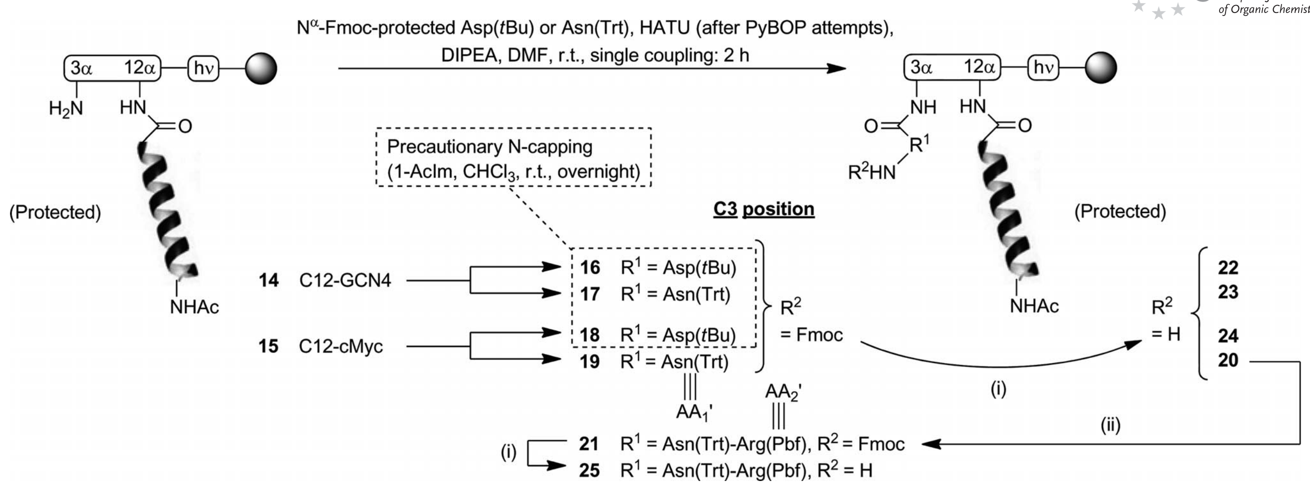

Scheme 3. From C12 monomers to C3–C12 dimers through key attachment of the first C3 residue. Reagents and conditions: (i) Piperidine in DMF (20% v/v), r.t., triple deprotection: 2 + 5 + 15 min. (ii) N^{α}-Fmoc-protected Arg(Pbf), PyBOP, DIPEA, DMF, r.t., double coupling: 2.5 + 5 h.

Different batches of Alloc-deprotected resins **14** and **15** were C3 derivatized with either protected aspartate or protected asparagine towards compounds **16**–**19** (Scheme 3). Manual attachment of the first residues again preceded automated peptide assembly, and couplings were carefully evaluated. RP-HPLC equipped with the C18/100 Å stationary phase allowed the consumption of starting materials **14** and **15** to be assessed. Surprisingly, a double PyBOP-mediated procedure failed to quantitatively derivatize the C3 amino group, in contrast to the previous outcome at the hindered C12 appendage. Although the C3 position of the current scaffold has generally been considered the most reactive site, accessibility might be significantly impaired by the proximal, side chain protected first strand present in this particular constrained design. Further PyBOP-based attempts were unsuccessful. Gratifyingly, application of the renowned HATU {1-[bis(dimethylamino)methylene]-1*H*-1,2,3-triazolo[4,5-*b*]pyridinium hexafluorophosphate 3-oxide} reagent provided increased coupling. However, whereas quantitative conversion of **15** into **19** was suggested by RP-HPLC and MALDI-TOF-MS (see Figure S20, Supporting Information), subsequent N^{α}-Fmoc deprotection still indicated the presence of contaminating starting material **15** (see Figure S22, Supporting Information). Double, perhaps triple, HATU coupling might therefore be considered for future research. Liberation of the N^{α}-amino group restored the proper eluting behavior and confirmed derivatized **20** as the major compound. Additionally, prior purification of samples by analytical RP-HPLC and subsequent lyophilization enhanced the crystallinity of the solid spots, improving MALDI-TOF-MS analysis.[63] Whereas data indicate preferential application of the α-cyanohydroxycinnamic acid matrix for analyzing previous, monomeric compounds, monitoring of the current C3 manipulation is better accommodated by 2,5-dihydroxybenzoic acid.

Considering these challenges, automated generation of the second strand might compromise significant steric constraints. Satisfyingly, in a preliminary test reaction it was shown that manual PyBOP-mediated attachment of a subsequent arginine residue at compound **20** provided straightforward formation of **21**. Although confirming particular demands of the constrained C3 position, a single residue seemed to sufficiently protrude for reliable further derivatization by the automated procedure. Remaining resins **16**–**18** were precautionary N capped by 1-AcIm prior to N^{α}-Fmoc deprotection to yield **22**–**24**, respectively. At this pivotal C3 position, once again the C4/300 Å stationary phase demonstrated general compatibility with all intermediates, which vouches for its superior verification and monitoring (see Supporting Information for RP-HPLC details and tabular summary: Table S5).

Relying on the satisfying synthesis of the monomeric intermediates, the current procedure was further exploited for the automated generation of the second peptide strand at the C3 position (Scheme 4). Synthetic feasibility could however be abrogated by the particular polarity and complexity of the macromolecular targets. Bearing structural similarities with so-called helical bundles, interchain interactions between both peptides could render aggregated strands inaccessible for adequate chain elongation.[42,64] Attempting to continue the monitoring strategy, samples were again subjected to RP-HPLC and MALDI-TOF-MS. Not surprisingly, incorporation of five additional residues at **25** definitely prevented proper elution on both the C18/100 Å and C4/300 Å stationary phase and detection by MALDI-TOF-MS.

... to C3–C12 Dimeric Peptidosteroids

Further attention was therefore immediately focused on subsequent acidic deprotection towards the desired, dimeric peptidosteroid compounds (Scheme 4). RP-HPLC and MALDI-TOF-MS analysis benefits from liberation of the numerous hydrophilic side chain functionalities. Although aromatic substitution by the liberated electrophiles[65] could significantly alter cleavage efficiency, resemblance of the employed photocleavable linker to the Rink amide {4-[(2,4-

dimethoxyphenyl)(Fmoc-amino)methyl]phenoxyacetic acid} and HMPB [4-(4-hydroxymethyl-3-methoxyphenoxy)butyric acid] linkers supported its acid stability.[66] Both compound recovery and integrity could be compromised by (the combination of) increased photostability, altered reactivity profile, and/or premature loss. Thus, to avoid the incontrollable occurrence of side reactions at the photolabile linker and the loss of precious compounds at this advanced stage, application of an inverse photolysis–acidolysis protocol was elaborated without further assessment of acidolytic linker cleavage. Upon the usual UV cleavage of side chain protected samples **26**–**29** in ACN (acetonitrile), the resulting opaque solutions were separated from the resin, and the evaporated material was subjected to the TIS (triisopropylsilane) containing acidolytic cocktail at room temperature for ca. 2 h. Upon concentration[67] and Et_2O trituration, flocculation seemed to benefit from warming of the samples to room temperature and a short (<1 min) period of sonication and intense vortexing. Consistent with the multitude of side chain protected residues in general and arginine-protecting Pbf (2,2,4,6,7-pentamethyldihydrobenzofuran-5-sulfonyl) groups in particular, incomplete deprotection was observed in the RP-HPLC and MALDI-TOF-MS data. To ensure complete deprotection, yet prevent decomposition, either 50 °C for 4 h or 60 °C for 2.5 h was applied to these partially deprotected compounds. Figure 4 (a) and (b) shows the excellent MALDI-TOF-MS and RP-HPLC data of crude precipitate **31**. Desired peptidosteroid dimer **31** was obtained as the major component, mainly contaminated by an acceptable amount of the C3-capped deletion sequence, which was anticipated from the above-discussed experiments.[68] Comparable results were obtained for the larger, GCN4-containing conjugates **32** and **33**.

Considering the relevance of the cMyc-Max heterodimer, further attention was focused on peptidosteroid **31**. In contrast to straightforward single (3 h) irradiation of analytical resin samples in small test tubes, scaled photolysis requires a careful experimental setup. In view of the generally observed opacity of samples containing larger compounds upon UV cleavage in ACN, solubility issues might hamper the efficient release of our hydrophobic, side chain protected peptidosteroids. Therefore, the influence of different solvents on the photolytic outcome was shortly assessed. ACN, EtOH, and acetone provided satisfying results, whereas samples in THF, dioxane (+2% DMSO) and *i*PrOH showed lower purity. Direct exposure of the floating resin to UV irradiation and/or generation of radical species might account for complete degradation in $CHCl_3$.[69] Considering the particular demands of our fully protected macromolecular conjugates, EtOH was selected over usually employed ACN for further experiments. While matching the desirable intermediate boiling point, decreased sample opacity indicated an enhanced solubility. The sufficiently low volatility of this (regularly replenished) solvent must prevent complete evaporation and minimize potential risks of directly irradiating dry resin/compound with intense UV light.[56] Peptide integrity further benefitted from several successive, rather short (max. 4 h) periods of photolysis with intermediate isolation, while providing sufficient cleavage recovery. Although extensive rounds of UV cleavage might be tempting yield-wise, RP-HPLC evaluation indicated an appreciable decrease in compound liberation in later samples, with a relative increase in contaminating species.

After single reagent B deprotection of cleaved **27** at an elevated temperature overnight, crude **31** was obtained in

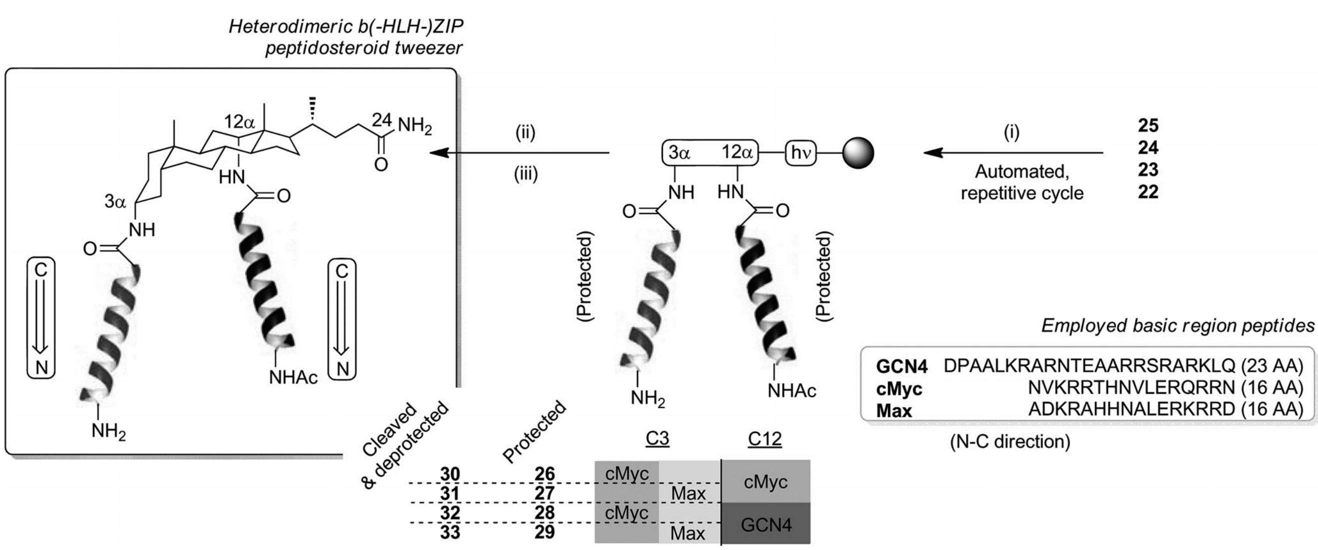

Scheme 4. Towards the final C3–C12 dimers in a 2×2 b(-HLH-)ZIP peptidosteroid library format. Reagents and conditions: (i) Until completion: (a) N^{α}-Fmoc-protected residue, HBTU, DIPEA, NMP (+ DMF trace), r.t., single coupling: 3 h; (b) piperidine in NMP (40% v/v), r.t., triple deprotection: 2 + 5 + 15 min. (ii) UV-light irradiation (365 nm) either on small scale (ACN, single cleavage: 3 h) or preparatory scale (EtOH, triple cleavage: 3.5 + 2.5 + 3.5 h). (iii) Reagent B (88% v/v TFA + 5% H_2O + 5% phenol + 2% TIS) under various conditions (small scale: r.t. for ca. 2 h + 50–60 °C for 2.5–4 h; or preparatory scale: 60 °C overnight) (see Experimental Section for details).

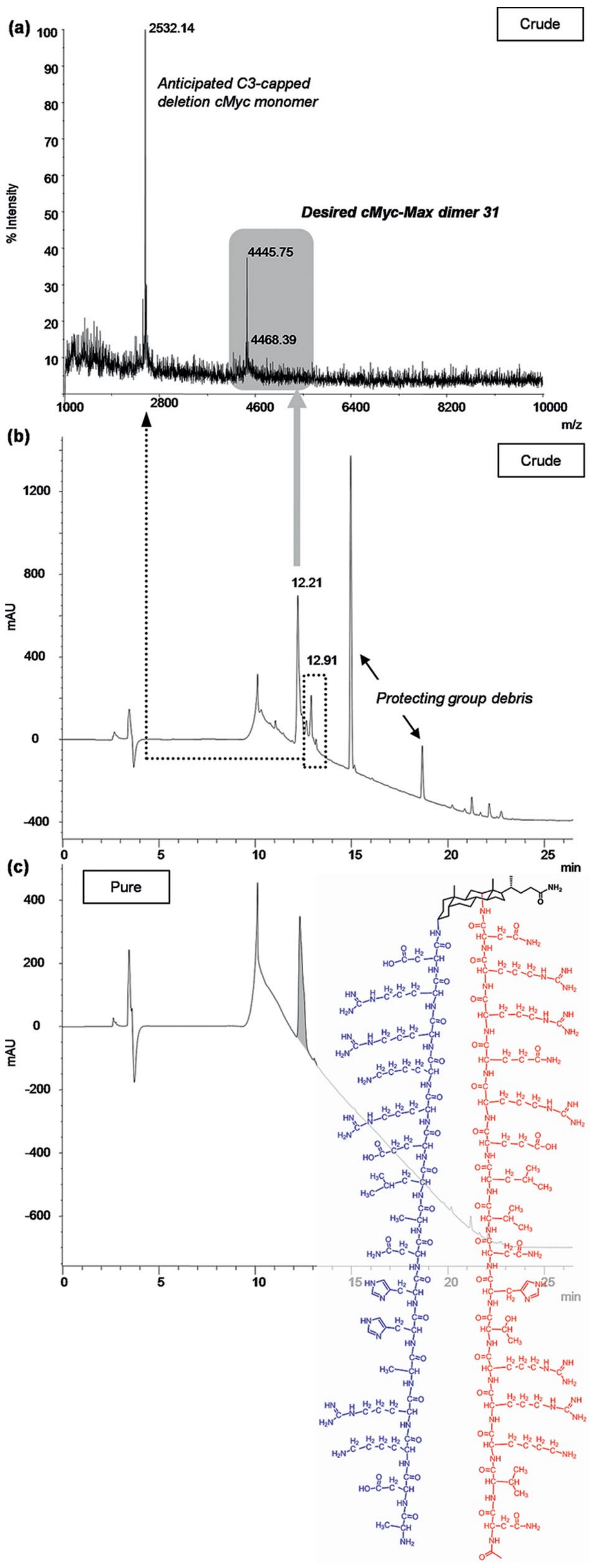

Figure 4. The first miniature cMyc-Max peptidosteroid tweezer model: (a) MALDI-TOF-MS (DHB) and (b) RP-HPLC (C18/100 Å, 214 nm, gradient 1)[58] of *crude* **31**, isolated after treatment with reagent B for ca. 2 h at r.t. + an additional 4 h at 50 °C. (c) RP-HPLC (C18/100 Å, 214 nm, gradient 1)[58] and complete structure of *purified* **31** (calcd. EM 4443.6, MW 4446.1; C3-NHAc capped deletion monomer: calcd. EM 2530.5, MW 2532.0).

62% isolated yield (as the TFA salt) over the photolysis–acidolysis steps. As the main contaminant, the defective C3-capped monomer showed a pronounced difference in retention time. Obtained in satisfying integrity according to Figure 4 (c), a finishing RP-HPLC purification of the crude material yielded our first miniature cMyc-Max tweezer model.

Conclusions

The potential of cMyc-Max downsizing was noticed shortly after its discovery in the 1990s.[26] Peptide miniatures as TF mimics might rival engineered protein or oligonucleotide approaches in terms of biostability/availability, yet outscore small-molecule, intercalator, or minor groove approaches in terms of target selectivity/generality.[18]

Prior establishment of a preparatory methodology is however a prerequisite for experimental evaluation of attractive designs, preferably approached by a library format. A simple SPPS strategy proved viable for the sequential generation of basic region peptides at the C12 and C3 positions of the scaffold module, thereby covalently restraining the appendages. Accommodated by a key NHAlloc protectant at the pivotal C3 position, both homo- and heterodimeric peptidosteroids were assembled by standard Fmoc/*t*Bu chemistry through automated procedures. Enabled by the facilitated photolytic release of minute samples at regular stages, an elaborate monitoring strategy focused on dedicated RP-HPLC and MALDI-TOF-MS analysis of side chain protected intermediates. Comprising recognition sequences of the natural GCN4, cMyc, and Max proteins, batch-wise incorporation of two basic region peptides at each scaffold position in a 2×2 combination design efficiently furnished a unique collection of first generation b(-HLH-)ZIP peptidosteroid models. Non-interfering with the binding process, the C24 handle might further be used to introduce measurable or switchable modules, which is desirable for advanced applications in the postgenomic era with a chemical biology mindset.[17]

Implementation of the here-reported solid-phase procedures into a parallel library setup should maximize the odds to identify recognition tendencies, facilitate the rationalization of design clues, and accelerate the miniaturization of the enigmatic loop-type TF class. Now equipped with a synthetic platform, current prototype contribution supplements the paucity of literature precedents, gives a taste of the many opportunities ahead, and provides a methodological framework from which systematic refinements can depart.

Experimental Section

General Information: All organic solvents and chemical reagents were acquired from commercial sources and used without further purification or drying. Extra-dry DMF (*N*,*N*-dimethylformamide; with molecular sieves, H_2O <50 ppm) was used during manual couplings and manual Fmoc deprotections. When utilizing this solvent for resin washing and during robot-assisted automated SPPS, peptide synthesis grade was used. The same applies for NMP. HPLC grade quality was employed for all other organic solvents (involved in, e.g., washing, color testing, Alloc/Boc deprotection, UV Fmoc determination, NAc capping, and photolysis). H_2O met the Milli-Q grade standard. DIPEA (*N*,*N*-diisopropylethylamine) was supplied as redistilled (i.e., dry), whereas tetrakis(triphenylphosphane)palladium(0) was 99% pure (Aldrich). TentaGel NH_2 resin (90 µm, manufacturer's loading: 0.28 mmol g^{-1}) was obtained from Merck Novabiochem. All chiral α-amino acids used in this paper possessed the L-configuration. Throughout this work, N^{α}-Fmoc-protected residues with standard acid-sensitive side chain PGs were used: Asp(O*t*Bu) [D], Glu(O*t*Bu) [E], His(Trt) [H], Lys(Boc) [K], Asn(Trt) [N], Gln(Trt) [Q], Arg(Pbf) [R], Ser(*t*Bu) [S], Thr(*t*Bu) [T]. Adapted from Holmes et al., photocleavable linker **2** was synthesized prior to the present work and employed as such.[44,45] The same applies to our steroid scaffold building block **1**.[40]

Automated peptide synthesis was performed on a fully-automated SYRO Multiple Peptide Synthesizer robot, equipped with a vortexing unit for the 24-reactor block (MultiSynTech GmbH). Reactions were open to the atmosphere, executed at ambient temperature and shielded from light. Photolysis was carried out on a small scale with a 4 W Bioblock Scientific compact UV lamp, set at 365 nm. For large scale cleavage, a 451 W UV ACE glass incorporated 7225–34 immersion lamp equipped with a Schott WG320 UV cut-off filter was used. The bead suspension was thereby continuously agitated by N_2 bubbling, and the solvent was regularly replenished to prevent direct resin irradiation by complete solvent evaporation. All samples were cleaved at a distance of ca. 1 cm from the lamp.

RP-HPLC analysis and purification was performed with diode array detection by using a Phenomenex Luna C18 (2) 100 Å column (250 × 4.6 mm, 5 µ, at 35 °C) or a Phenomenex Jupiter C4/300 Å column (250 × 4.6 mm, 5 µ, at 35 °C) by applying a flow rate of 1.0 mL min^{-1}. Signals at 214, 254, 280, 310, and 360 nm were simultaneously detected. Through a binary solvent system composed of (A =) H_2O + TFA (0.1%) and (B =) ACN as the mobile phase, linear gradient elution was performed: after injection (and shown in the chromatographic output) the column was flushed with x% B for 3 min, followed by a linear increase in B (vs. A) to 100% in y min, finishing by flushing with 100% B for 5 min, after which the gradient was returned to x% B in 0.5 min, concluding the cycle by flushing with x% B for 3 min. Gradient 1 refers therein to (x,y) = (0, 15), or a 0 to 100% linear increase in B (vs. A) over 15 min. Gradient 2 refers therein to (x,y) = (75, 15), or a 75 to 100% linear increase in B (vs. A) over 15 min. In addition to these standard gradients, all others follow the same profile. For brevity, only the linear increase in B vs. A is quoted in the remainder of this manuscript. ESI-MS spectra were recorded with a quadrupole ion trap LC mass spectrometer, equipped with electrospray ionization. MeOH/H_2O (4/1 ± 0.1% formic acid) was used as carrier solution. All data were collected in the positive mode, at a capillary temperature of 250 °C. MALDI-TOF-MS spectra were acquired with a high-performance nitrogen laser (337 nm), using the positive and reflectron mode with delayed extraction. All measurements were calibrated against MePEOH ($M_n \approx 2000$, PD = 1.06), spotted from a MeOH (2 mg mL^{-1}) solution. The following matrix solutions were utilized (made in microtubes, stored in freezer, carefully defrosted and homogenized upon use): DHB: 2,5-dihydroxybenzoic acid (98.0% pure, 10 mg) + ACN (500 µL) + H_2O (470 µL) + $TFA_{aq.}$ (30 µL, 3%); α-CHCA: α-cyano-4-hydroxycinnamic acid (99% pure, 10 mg) + ACN (500 µL) + H_2O (400 µL) + $TFA_{aq.}$ (100 µL, 3%). LC-(TIC)-MS analysis (reverse-phase) was performed with diode array detection by using a Phenomenex Luna C18 (2) 100 Å column (250 × 4.6 mm, 5 µ, at 35 °C), with hyphenation to an ESI single quadrupole MS detector type VL. A flow rate of 1.0 mL min^{-1} was applied. UV detection was done at 214, 254, 280, 310, and 360 nm simultaneously, and mass detection operated in the positive mode. Through a binary solvent system composed of (A =) H_2O + HCOOH (0.1%) or H_2O + NH_4OAc (5 mM) and (B =) ACN as the mobile phase, linear gradient elution was performed by applying gradients similar to the above RP-HPLC profiles (yet with shorter 2 min preflushing phase).

It is noted that compound numbers were used interchangeably between the solid-supported molecules and the liberated counterparts. Compounds were released (and analyzed) as C24 carboxamides upon UV irradiation of the corresponding resin. Unless stated otherwise, all analytical data refer to crude (i.e., non-RP-HPLC-purified) samples, which were, at most, subjected to trituration with Et_2O. Empirical formulae refer to neutral molecules.

Standard Procedure for Small-Scale Photolytic Cleavage: Either aiming for analytical verification/monitoring or proceeding towards compound isolation, a resin sample (1–5 mg) was transferred to a miniature glass test tube (600 µL, 35 × 6 mm Ø) and suspended in an appropriate solvent (4–8 drops), usually ACN or EtOH. The tube was flushed with argon and sealed with a septum. Placed near-horizontally at a distance of ca. 1 cm from the small-scale UV lamp (365 nm), the beads were irradiated for 3 h, with occasional manual homogenization of the resin suspension. Using a glass syringe with a narrow bore cemented needle, the resulting solution was carefully separated from the resin, ready for further manipulation or analysis.

Synthesis of Resin-Bound Steroid Scaffold Starting Constructs

Coupling of Photocleavable Linker 2 to TentaGel NH_2 Resin → Construct 3: Weighed in a fritted glass reactor, TentaGel NH_2 resin (1.0 g, manufacturer's loading: 0.28 mmol g^{-1}, 0.28 mmol) was preswollen in dry DMF (10 mL) for 1 h. After filtration under reduced pressure, the beads were resuspended in dry DMF (4 mL) and photocleavable linker **2** (437.3 mg, 3 equiv.) was added, followed by dry DIPEA (280 µL, 6 equiv.) and dry DMF (3 mL). Upon addition of PyBOP (437.3 mg, 3 equiv.) and dry DMF (3 mL), the reaction vessel was flushed with argon, wrapped in foil, and agitated for 3 h at room temperature. During agitation, complete dissolution of the photocleavable linker was observed, which generated an intense orange mixture. Excess amount of the reagents and the solvent were removed by filtration under reduced pressure, and the resin was extensively washed with DMF, ACN, and DCM. After an additional DMF washing step, the reaction was repeated, agitating for 5 h. TNBS test:[47] colorless (pale orange after ca. 30–60 min as a result of test-induced NHFmoc deprotection); NF31 test:[48] pale pinkish-colorless (TentaGel NH_2 starting resin: either intense orange or intense red).

NHFmoc Deprotection of Construct 3: After an initial DMF washing step, resin **3** (0.28 mmol) was successively treated for 2, 5, and 15 min with a piperidine solution in DMF (20% v/v, 6 mL) at ambient temperature by applying intermediate filtration under reduced pressure and washing with DMF. The final resin was additionally washed with ACN and DCM. TNBS test:[47] intense orange (coloration delayed as a result of hindrance by the α-methyl group); NF31 test:[48] intense dark red.

Coupling of Steroid Scaffold 1 to Solid-Supported Photocleavable Linker → Compound 4: The resulting construct (0.28 mmol), preswollen with an additional washing step with dry DMF, was suspended in dry DMF (6 mL). Steroid scaffold **1** (193.3 mg, 1.2 equiv.) and dry DIPEA (115 µL, 2.4 equiv.) were added, followed by dry DMF (3 mL). Addition of PyBOP (175.0 mg, 1.2 equiv.) and dry DMF (3 mL) completed the reaction mixture. Rapid dissolution of the solid compounds was observed, and the argon-flushed vessel was gently agitated and shielded from light. Upon overnight reaction at room temperature, the excess amounts of the reagents and the solvent were removed under reduced pressure, and the solid-phase beads were extensively washed with DMF, ACN, and DCM. Single overnight coupling was followed by a precautionary N-capping step: the resulting resin was washed with $CHCl_3$ as a preswelling step, followed the by addition of $CHCl_3$ (8 mL) and 1-AcIm (308.5 mg, 10 equiv.). The argon-flushed reaction mixture was gently agitated overnight at room temperature and shielded from light. The solution was discarded by filtration under reduced pressure, and the resin was extensively washed with $CHCl_3$. TNBS[47] and NF31 test:[48] colorless (executed before capping). A small sample was photolytically cleaved (365 nm) for analysis. ESI-MS [E(xact) M(ass) calcd. for $C_{33}H_{55}N_3O_5$ 573.4 (M(ol.)W(t.) 573.8)]: *m/z* (%) = 474.2 (100) $[M – Boc]^+$, 596.2 (28) $[M + Na]^+$, 573.7 (10) $[M + H]^+$, 1146.6 (2) $[2M + H]^+$.

C12 NHBoc Deprotection of 4 → Compound 5: Following an initial washing/preswelling step with DCM, resin **4** (0.28 mmol) was successively treated with a TFA solution in DCM (20% v/v, 6 mL) for 2, 5, and 15 min at room temperature. DCM was used for intermediate washing, and the final resin was further purified by consecutive rinsing with DCM, DMF, DIPEA/DMF (10% v/v), DMF, ACN, DCM, and Et_2O, removed by filtration under reduced pressure. The resin beads were thoroughly dried under high vacuum. TNBS test:[47] light orange after prolonged reaction (significant hindrance); NF31 test:[48] intense red. A small sample was photolytically cleaved (365 nm) for analysis. ESI-MS [EM calcd. for $C_{28}H_{47}N_3O_3$ 473.4 (MW 473.7)]: *m/z* (%) = 474.3 (100) $[M + H]^+$, 931.5 (6) $[2M – NH_3]^+$, 457.2 (4) $[M – NH_3]^+$. LC-TIC-MS [Luna C18/100 Å, gradient 1 (A = $HCOOH_{aq.}$)]: t_R = 11.8 min.

Coupling of the First Residue to the C12 Position of 5 → Compounds 6–7: Two portions of scaffold-bearing resin **5** (50 mg each, theoretical loading calcd. from TentaGel: 0.23 mmol g^{-1}, 0.0115 mmol) were weighed in fritted syringe reactors (5 mL), washed with dry DMF, filtered under reduced pressure, and resuspended in dry DMF (1 mL). Dry DIPEA (8.0 µL, 4 equiv.), either NHFmoc-protected Gln(Trt) or Asn(Trt) (28.1 or 27.4 mg, respectively, 4 equiv.) and PyBOP (23.9 mg, 4 equiv.) were consecutively added, observing rapid dissolution of the latter. The reactors were flushed with argon and wrapped in foil. After vortexing the reaction mixtures at room temperature for 4 h, the excess amounts of the reagents and the solvent were removed under reduced pressure, and the resins were washed with DMF, ACN, and DCM. After an additional washing step with dry DMF, the couplings were repeated. TNBS test:[47] colorless (pale orange after ca. 30–60 min, but biased by the hindrance in the starting material on the one hand, yet TNBS test induced premature NHFmoc deprotection on the other hand); NF31 test:[48] pale pinkish-colorless. UV Fmoc[70] estimated loading: For **6**: 0.072 mmol g^{-1}; for **7**: 0.096 mmol g^{-1}. A small sample was photolytically cleaved (365 nm) for analysis. For **6**: ESI-MS [EM calcd. for $C_{67}H_{79}N_5O_7$ 1065.6 (MW 1066.4)]: *m/z* (%) = 1066.2 (23) $[M + H]^+$, 1088.5 (77) $[M + Na]^+$, 1105.6 (15) $[M + K]^+$, 243.2 (100) $[Trt]^+$. LC-MS [Luna C18/100 Å, gradient 2 (A = $NH_4OAc_{aq.}$)]: t_R = 16.6 min. RP-HPLC (Luna C18/100 Å, gradient 2): t_R = 19.1 min. For **7**: ESI-MS [EM calcd. for $C_{66}H_{77}N_5O_7$ 1051.6 (MW 1052.4)]: *m/z* (%) = 1052.0 (34) $[M + H]^+$, 1074.6 (50) $[M + Na]^+$, 1090.6 (13) $[M + K]^+$, 243.2 (100) $[Trt]^+$.

NHFmoc Deprotection of 6–7 → Compounds 8–9: Before automated peptide synthesis, resins **6** and **7** were manually NHFmoc deprotected by using the procedure described above. After deprotection, the resins were dried under high vacuum. TNBS test:[47] rapidly intense orange/reddish; NF31 test:[48] rapidly intense dark red. A small sample was photolytically cleaved (365 nm) for analysis. For **8**: ESI-MS [EM calcd. for $C_{52}H_{69}N_5O_5$ 843.5 (MW 844.1)]: *m/z* (%) = 844.4 (100) $[M + H]^+$, 867.6 (21) $[M + Na]^+$, 243.2 (60) $[Trt]^+$, 1688.0 (9) $[2M + H]^+$. RP-HPLC (Luna C18/100 Å, gradient 1): t_R = 18.4 min. For **9**: ESI-MS [EM calcd. for $C_{51}H_{67}N_5O_5$ 829.5 (MW 830.1)]: *m/z* (%) = 830.4 (100) $[M + H]^+$, 852.5 (52) $[M + Na]^+$, 243.2 (79) $[Trt]^+$, 1659.3 (6) $[2M + H]^+$, 1672.7 (4) $[2M + Na]^+$. RP-HPLC (Luna C18/100 Å, gradient 1): t_R = 18.4 min.

Robot-Assisted SPPS of Side Chain Protected b(-HLH-)ZIP Peptidosteroids

Automated Synthesis of (Side Chain Protected) C12 Peptidosteroid Intermediates: Compounds 8–9 → Compounds 10–11: Resins **8** (30.4 mg, 0.07 mmol g^{-1}, 2.1 µmol scale) and **9** (30.1 mg, 0.1 mmol g^{-1}, 3 µmol scale) were transferred to smaller (2 mL) syringe reactors. Experimental loadings of these resins were calculated from the actual values of UV-Fmoc quantified precursors **6** and **7** (see data above), translating to 0.07 and 0.1 mmol g^{-1} for **8** and **9**, respectively. A detailed overview of the automated cycle program is included in the Supporting Information (Table S3). In summary, after 15 min of preswelling in NMP (312 µL), the resin beads were filtered, and the desired peptide sequences were generated from the C to N terminus through a repetitive coupling–deprotection cycle by using the Fmoc/*t*Bu SPPS methodology: NMP solutions of N^{α}-Fmoc-protected residues (0.5 M), DIPEA (0.9 M), and HBTU (0.5 M, + 5% DMF) were sequentially added in equal volumes (104 µL each) to resins **8** and **9**. The resulting coupling mixtures (312 µL, 0.16 M of active species, 25 and 17.5 equiv. respectively, + 2% DMF) were allowed to react for a 3-h single coupling period, with gentle vortexing at regular intervals, after which the excess amount of the reagents and the solvent were removed under reduced pressure, and the resins were extensively washed with NMP (9 × 312 µL). Translated from the manual procedure described above, subsequent automated NHFmoc deprotection was effected by successive treatment (2, 5, and 15 min) of the resin beads with a piperidine solution in NMP (40% v/v, 312 µL), with filtration under reduced pressure and extensive washing with NMP (6 × 312 µL) after every deprotection cycle. These coupling–deprotection steps were repeated until completion. In addition to the intermediate samples taken for the semi-online monitoring purposes as described, to evaluate the complete sequence a small sample was photolytically cleaved (365 nm) for analysis. For **10**: MALDI-TOF-MS [(α-CHCA): EM calcd. for $C_{278}H_{412}N_{48}O_{56}S_6$ 5510.9 (MW 5514.9)]: *m/z* = 5537.6 $[M + Na]^+$, 5553.5 $[M + K]^+$. RP-HPLC (Jupiter C4/300 Å, gradient 1): t_R = 23.2 min. For **11**: MALDI-TOF-MS [(α-CHCA): EM calcd. for $C_{285}H_{369}N_{41}O_{43}S_5$ 5213.7 (MW 5217.6)]: *m/z* = 5238.7 $[M + Na]^+$, 5255.8 $[M + K]^+$. RP-HPLC (Jupiter C4/300 Å, gradient 1): t_R = 23.1 min.

Manual Incorporation of the N-Terminal Acetyl Cap at the C12 Strand of (Side Chain Protected) Peptidosteroid Intermediates 10–11 → Compounds 12–13: In the same tubes (2 mL) employed during the automated peptide assembly, resin **10** (2.1 µmol) and **11** (3.0 µmol) were suspended in $CHCl_3$ (200 µL each) and 1-AcIm (2.4 and 3.3 mg, respectively, 10 equiv.) was added. Flushed with argon and wrapped in foil, the reactors were agitated overnight at room temperature. The excess amounts of the reagent and the solvent were removed under reduced pressure, and the resins were washed with $CHCl_3$, DMF, MeOH, and DCM. A small sample was photolytically cleaved (365 nm) for analysis. For **12**: MALDI-TOF-MS [(α-CHCA): EM calcd. for $C_{280}H_{414}N_{48}O_{57}S_6$ 5552.9 (MW 5557.0)]: *m*/*z* = 5304.8 [M – Pbf + H]$^+$. For **13**: MALDI-TOF-MS [(α-CHCA): EM calcd. for $C_{287}H_{371}N_{41}O_{44}S_5$ 5255.7 (MW 5259.6)]: *m*/*z* = 4755.1 [M – 2Pbf + H]$^+$, 5007.3 [M – Pbf + H]$^+$, 5029.9 [M – Pbf + Na]$^+$, 5283.2 [M + Na]$^+$, 5297.4 [M + K]$^+$. RP-HPLC (Jupiter C4/300 Å, gradient 1): t_R = 23.4 min.

Manual Removal of the C3 NHAlloc Protecting Group in (Side Chain Protected) Peptidosteroid Intermediates 12–13 → Compounds 14–15: Prior to the reaction, resins **12** and **13** were additionally washed with DCM and Et_2O, followed by careful drying under high vacuum. Experimental loadings of these resins were calculated from the actual values of UV-Fmoc quantified precursors **6** and **7** (see data above), translating to 0.053 and 0.07 mmol g^{-1} for **12** an **13**, respectively. Progressing towards our 2 × 2 solid-phase library setup, these resins were both divided into two fritted syringe reactors to obtain two batches of each resin (**12**: 20.6 mg, 1.1 µmol and 11.9 mg, 0.63 µmol; **13**: 14.7 mg, 1.0 µmol and 25.6 mg, 1.8 µmol). As illustrated for the third batch, the following chemicals were sequentially added: DCM (100 µL), morpholine (8.1 µL, 90 equiv.), Bu_3SnH (2.7 µL, 10 equiv.), $Pd(PPh_3)_4$ (1.3 mg, 1 equiv.), and DCM (150 µL). The resulting yellow-orange reaction mixtures were flushed with argon, shielded from light and vortexed at room temperature for 2 h. The excess amounts of the reagents and the solvent were removed by filtration under reduced pressure, and the resins were thoroughly washed with DCM, DMF, MeOH, and DCM. TNBS test:[47] intense orange/red after ca. 30 min. A small sample was photolytically cleaved (365 nm) for analysis. For **14**: MALDI-TOF-MS [(DHB): EM calcd. for $C_{276}H_{410}N_{48}O_{55}S_6$ 5468.9 (MW 5472.9)]: *m*/*z* = 5494.1 [M + Na]$^+$, 5510.1 [M + K]$^+$, 5218.0 [M – Pbf + H]$^+$. RP-HPLC (Luna C18/100 Å, gradient 1): t_R = 23.1 min. For **15**: MALDI-TOF-MS [(DHB): EM calcd. for $C_{283}H_{367}N_{41}O_{42}S_5$ 5171.6 (MW 5175.5)]: *m*/*z* = 5196.7 [M + Na]$^+$, 5214.5 [M + K]$^+$, 4944.3 [M – Pbf + Na]$^+$, 4920.5 [M – Pbf + H]$^+$. RP-HPLC (Luna C18/100 Å, gradient 1): t_R = 22.2 min.

Manual Introduction of the First Residue of the Second Strand at the Available C3 NH_2 Group in (Side Chain Protected) Peptidosteroid Intermediates 14 and 15 → Compounds 16–17 and 18–19: The obtained NHAlloc-deprotected resins were washed with dry DMF prior to reaction. Again illustrated for the above batch (towards **19**), the resin beads were resuspended in dry DMF (60 µL), followed by consecutive addition of dry DIPEA (0.7 µL, 4 equiv.), NHFmoc-protected Asn(Trt) (2.4 mg, 4 equiv.), PyBOP (2.0 mg, 4 equiv.), and dry DMF (60 µL). The solid reagents readily dissolved, and the reaction mixture was flushed with argon, shielded from light, and vortexed at room temperature for 2 h. After the reaction, the excess amounts of the reagents and the solvent were removed by filtration under reduced pressure, and the resin was rinsed with DMF, MeOH, and DCM. The procedure was repeated (reaction for 3 h), yet incomplete reaction was observed upon analysis, even after further repetition. Although the inferior analytical outcome of the other batches prevented conclusive interpretation, diagnostic results were obtained for **19**, as discussed above and evidenced in the Supporting Information. Fortunately, satisfying conversion was obtained by a similar 2-h (single) treatment with HATU as the coupling reagent (1.6 mg, 4 equiv.). A small sample was photolytically cleaved (365 nm) for analysis. For **19**: MALDI-TOF-MS [(DHB): EM calcd. for $C_{321}H_{397}N_{43}O_{46}S_5$ 5749.9 (MW 5754.2)]: *m*/*z* = 5776.4 [M + Na]$^+$, 5792.3 [M + K]$^+$. RP-HPLC (Jupiter C4/300 Å, gradient 1): t_R = 23.5 min. In contrast to resin **19**, which was further derivatized as presented below, resins **16**–**18** were subjected to precautionary N-capping (adopting the above-described procedure) of potentially underivatized amino groups at the C3 scaffold position prior to Fmoc removal of the appended residue and automated elongation of the second strand, thereby securing the original lack of decisive monitoring.

Manual Test Introduction of the Second Residue of the Second Strand at (Side Chain Protected) Peptidosteroid Intermediate 19 (via 20) → Compound 21: To assess the influence of steric impediment, resin-bound compound **19** was manually derivatized with an additional residue. First, the NHFmoc protectant was removed as described to yield N^{α}-deprotected compound **20**. A small sample was photolytically cleaved (365 nm) for analysis. For **20** ($C_{306}H_{387}N_{43}O_{44}S_5$, calcd. EM 5527.8, MW 5531.9): RP-HPLC (Luna C18/100 Å, gradient 1): t_R = 22.7 min. After an initial washing step with dry DMF, resulting resin **20** was resuspended in dry DMF (100 µL) and NHFmoc-protected Arg(Pbf) (2.7 mg, 4 equiv.), dry DIPEA (1.4 µL, 8 equiv.), and PyBOP (2.0 mg, 4 equiv.) were added. The reaction was further homogenized by additional DMF (20 µL), flushed with argon, shielded from light, and vortexed for 2.5 h at ambient temperature. The excess amount of the reagents and the solvent were removed under reduced pressure, and the reaction was repeated (5 h). A small sample was photolytically cleaved (365 nm) for analysis. For **21** ($C_{340}H_{425}N_{47}O_{50}S_6$, calcd. EM 6158.0, MW 6162.7): RP-HPLC (Jupiter C4/300 Å, gradient 1): t_R = 23.6 min.

Manual Deprotection of the NHFmoc Protecting Group of (Side Chain Protected) Peptidosteroid Intermediates 16–18 and 21 → Compounds 22–24 and 25: Before automated assembly of the second peptide strand at the C3 position of resins **22**–**24** and **25**, NHFmoc deprotection of **16**–**18** and **21**, respectively, was manually performed, by adopting the above-described procedure. A small sample was photolytically cleaved (365 nm) for analysis. For **24** ($C_{291}H_{380}N_{42}O_{45}S_5$, calcd. EM 5342.7, MW 5346.7): RP-HPLC (Luna C18/100 Å, gradient 2): t_R = 19.3 min. For **25**: An analytical sample was purified by RP-HPLC for MALDI-TOF-MS [(DHB): EM calcd. for $C_{325}H_{415}N_{47}O_{48}S_6$ 5936.0 (MW 5940.4)]: *m*/*z* = 5734.9 [M – Trt + K]$^+$, 5719.2 [M – Trt + Na]$^+$, 5697.3 [M – Trt + H]$^+$, 5444.0 [M – Trt – Pbf + H]$^+$. RP-HPLC (Luna C18/100 Å, gradient 2): t_R = 20.6 min.

Automated Synthesis of (Side Chain Protected) C12–C3 Peptidosteroid Dimers: Compounds 25 and 24–22 → Compounds 26 and 27–29: Prior to reaction, resins **25** and **24**–**22** were additionally washed with Et_2O, followed by careful drying under high vacuum and transferred to small (2 mL) syringe reactors. Experimental loadings of these resins were calculated from the actual values of UV-Fmoc quantified precursors **7** and **6** (see data above), translating to 0.067 and 0.051 mmol g^{-1} for **24**–**25** and **22**–**23**, respectively. These resins were subjected to the same automated procedure as described above (0.16 M of active species, 3-h single couplings), with scaled conditions (0.2–1.4 µmol scale). A detailed overview of the automated cycle program is included in the Supporting Information (Table S6).

Photolysis–Acidolysis towards Final Deprotected Peptidosteroids

Preparation of Final Analytical Samples of Side Chain Deprotected Peptidosteroids 30–33: Prior to UV cleavage, resins **26**–**29** were washed with Et_2O and dried under high vacuum. As described above, the resins (3–4 mg) were photolytically cleaved (3 h) in ACN, with occasional swirling of the resin suspensions. The resulting opaque whitish solutions were transferred to microtubes (1.5 mL), aided by MeOH and sonication. The solutions were evaporated under reduced pressure. The yellowish/white, oil-like residues were further dried under high vacuum. Reagent B (88% v/v TFA + 5% H_2O + 5% phenol + 2% TIS, 100 µL) was added to each residue, and the microtubes were sonicated. Appearance of an intense yellow color was rapidly observed. The samples were vortexed at room temperature for ca. 2 h. The mixtures were evaporated under reduced pressure and Et_2O (20 drops) was added (at room temperature) to the resulting orange residues, readily observing flocculation. After sonicating, intensely vortexing, and reflocculation, the microtubes were centrifuged (20 °C, 10 min, 4500 rpm). The clear supernatants were carefully removed with a narrow bore cemented glass syringe and the Et_2O washing was repeated. Residual Et_2O was removed by gentle argon flushing. The white-greyish solids were dissolved in MeOH (100 µL, sonication) and analysis demonstrated incomplete removal of side chain PGs as discussed. Therefore, the solutions were evaporated under reduced pressure and the acidolysis procedure was repeated, yet partially deprotected C12-cMyc–C3-Max **31** was heated at 50 °C for 4 h, whereas partially deprotected cMyc-cMyc **30**, GCN4-cMyc **32**, and GCN4-Max **33** were heated at 60 °C for 2.5 h. Satisfying results were obtained for compound **31**, **32**, and **33**, whereas compound **30** was sacrificed along the experimental optimizations. For **31**: Vide infra. For **32**: MALDI-TOF-MS [(DHB): EM calcd. for $C_{218}H_{386}N_{86}O_{56}$ 5105.0 (MW 5107.9)]: m/z = 5107.1 $[M + H]^+$, 5090.7 $[M - H_2O + H]^+$. RP-HPLC (Luna C18/100 Å, gradient 1): t_R = 12.5 min. For **33**: MALDI-TOF-MS [(DHB): EM calcd. for $C_{214}H_{374}N_{83}O_{56}$ 5002.9 (MW 5005.8)]: m/z = 5003.7 $[M + H]^+$, 4986.4 $[M - H_2O + H]^+$. RP-HPLC (Luna C18/100 Å, gradient 1): t_R = 12.5 min.

Scaled Preparation of Final Side Chain Deprotected cMyc-Max Peptidosteroid 31: As discussed above, further emphasis was put on cMyc-Max model **31**, for which a scaled photolysis–acidolysis was performed. Prior to reaction, resin **27** was additionally washed with DCM and Et_2O, followed by careful drying under high vacuum. The resin was transferred to a small fritted glass reactor. The experimental loading of this resin was calculated from the actual value of UV-Fmoc quantified precursor **7** (see data above), translating to 0.054 mmol g^{-1}, and cMyc-Max bearing resin **27** (18.2 mg, 0.983 µmol) was suspended in EtOH (2 mL). Left for 15 min to allow preswelling, this resin was irradiated by the large-scale UV lamp for 3.5 h, with N_2 bubbling for agitation. At regular intervals (ca. 1 h), EtOH (1 mL) was added to prevent complete evaporation. The resulting solution and combined washings (EtOH) were collected in a flask (100 mL), obtaining a yellowish oil-like residue upon evaporation. The procedure was repeated twice (2.5 and 3.5 h), and the batches were isolated in distinct flasks. Redissolved in MeOH, the isolates were transferred to smaller flasks (10 mL) and the solutions were evaporated. The resulting residues were dried under high vacuum. Flushed with argon and magnetically stirred, these batches were overnight treated with reagent B (1 mL each) at 60 °C, showing rapid dissolution of the residues. The mixtures were cooled to room temperature, toluene was added, and the solutions were evaporated under reduced pressure. The orange-brownish residues were further dried under high vacuum, and Et_2O was added at room temperature. The mixtures were sonicated, vortexed, and transferred to centrifuge tubes with additional Et_2O (total of 9 mL each), resulting in flocculation of white-greyish precipitates. The tubes were centrifuged (23 °C, 10 min, 5000 rpm), the supernatant was discarded, and the Et_2O trituration was repeated (2 mL). Redissolved in MeOH (aided by sonication), the obtained material was transferred in the original flasks (10 mL), evaporated under reduced pressure, and the solid residues were further dried under high vacuum. Crude, deprotected peptidosteroid **31** was obtained in 62% isolated yield (respectively 1.1 mg + 1.3 mg + 1.4 mg = 3.8 mg, 0.606 µmol, as TFA salt: 4446.1 + 16 TFA = MW 6270.4) over the photolysis–acidolysis steps. Upon analysis, the batches were dissolved in MeOH and pooled, proceeding towards RP-HPLC purification of an analytical sample (Luna C18/100 Å, linear increase of B vs. A from 0 to 100% over 30 min, 214 nm: t_R = 15.7 min). For **31**: MALDI-TOF-MS [(DHB): EM calcd. for $C_{190}H_{329}N_{76}O_{48}$ 4443.6 (MW 4446.1)]: m/z = 4445.1 $[M + H]^+$, 4428.2 $[M - H_2O + H]^+$. RP-HPLC (Luna C18/100 Å, gradient 1): t_R = 12.3 min.

Supporting Information (see footnote on the first page of this article): Details of the robot-assisted SPPS protocols, additional information of the monitoring/analytical efforts, and supporting data for compound evaluation (including overview tables, RP-HPLC chromatograms, and ESI/MALDI-TOF mass spectra).

Acknowledgments

This research was financially supported by Ghent University (BOF 011D16403) and the Research Foundation Flanders (FWO KAN 1.5.186.03; G.0347.04N). We gratefully thank Prof. Dr. José L. Mascareñas, Dr. M. Eugenio Vázquez, and Dr. Olalla Vázquez (University of Santiago de Compostela, Spain) for useful discussions during a short research stay in their laboratory. Suggestions from Prof. Takashi Morii (Kyoto University, Japan) are further acknowledged. Technical assistance by Jan L. Goeman is appreciated. Noël Hosten and Jos Van den Begin are thanked for the synthesis of the photocleavable linker.

[1] Selected reviews: a) P. P. Pandolfi, *Oncogene* **2001**, *20*, 3116; b) L. H. Hurley, *Nat. Rev. Cancer* **2002**, *2*, 188; c) J. E. Darnell Jr., *Nat. Rev. Cancer* **2002**, *2*, 740; d) M. S. Redell, D. J. Tweardy, *Drug Discovery Today Technol.* **2006**, *3*, 261; e) P. Brennan, R. Donev, S. Hewamana, *Mol. Biosyst.* **2008**, *4*, 909.

[2] Which consists of related isoforms such as c-Myc (cellular), v-Myc (viral), L-Myc (involved in lung carcinoma), and N-Myc (involved in neuroblastoma).

[3] C. Grandori, S. M. Cowley, L. P. James, R. N. Eisenman, *Annu. Rev. Cell Dev. Biol.* **2000**, *16*, 653.

[4] Selected reading: a) S. Pelengaris, M. Khan, G. Evan, *Nat. Rev. Cancer* **2002**, *2*, 764; b) E. V. Prochownik, *Expert Rev. Anticancer Ther.* **2004**, *4*, 289; c) M. Vita, M. Henriksson, *Semin. Cancer Biol.* **2006**, *16*, 318.

[5] While targeting the DNA–protein interface in the present work, several contributions interfere with the corresponding protein–protein contacts (particularly) through small-molecule (i.e., non-peptidic) disruptors, thereby corroborating the relevance of studying TFs while acknowledging the associated difficulties. Selected reviews: a) D. L. Boger, J. Desharnais, K. Capps, *Angew. Chem.* **2003**, *115*, 4270; *Angew. Chem. Int. Ed.* **2003**, *42*, 4138; b) W. C. Tse, D. L. Boger, *Chem. Biol.* **2004**, *11*, 1607; c) H. Arndt, *Angew. Chem.* **2006**, *118*, 4664; *Angew. Chem. Int. Ed.* **2006**, *45*, 4552; d) A. N. Koehler, *Curr. Opin. Chem. Biol.* **2010**, *14*, 331; e) S. J. Metallo, *Curr. Opin. Chem. Biol.* **2010**, *14*, 481.

[6] L. E. Canne, A. R. Ferré-D'Amaré, S. K. Burley, S. B. H. Kent, *J. Am. Chem. Soc.* **1995**, *117*, 2998.

[7] T. Morii, M. Simomura, S. Morimoto, I. Saito, *J. Am. Chem. Soc.* **1993**, *115*, 1150.

[8] The basic region, HLH region, and leucine zipper domain coexist in different combinations in a total of four folds. b-HLH and HLH-ZIP proteins complement the bZIP and b-HLH-ZIP types, with striking parallels between all of them. The b-HLH-ZIP proteins are closely related to the network of b-HLH counterparts, either being classified as class C vs. class A/B members in an HLH-focusing taxonomy (and HLH-ZIP = class D) or being allocated to the alternative zipper-type group: a) N. M. Luscombe, S. E. Austin, H. M. Berman, J. M. Thornton, *Genome Biol.* **2000**, *1*, 1; b) S. Jones, *Genome Biol.* **2004**, *5*, 1.

[9] a) C. O. Pabo, L. Nekludova, *J. Mol. Biol.* **2000**, *301*, 597; b) N. M. Luscombe, R. A. Laskowski, J. M. Thornton, *Nucleic Acids Res.* **2001**, *29*, 2860.

[10] The overall dimensions of an α-helix allow it to fit into the *major groove* in a number of ways. This variability explains the preference of natural proteins for targeting this wider groove over the narrower minor one. It accordingly accounts for the contrasting prevalence of *minor groove* targeting mimics, as their less ambiguous binding mode facilitates the rationalization of recognition/design principles. The synthetic polyamides of Dervan et al. are prominent examples thereof. A notable exception are the (mostly, if not all, bioengineered) zinc finger proteins binding in the major groove (with Pabo et al. as protagonist), for which an advanced level of insight and pairing control has been achieved. Selected reviews: a) P. B. Dervan, B. S. Edelson, *Curr. Opin. Struct. Biol.* **2003**, *13*, 284; b) S. Negi, M. Imanishi, M. Matsumoto, Y. Sugiura, *Chem. Eur. J.* **2008**, *14*, 3236; c) A. Klug, *Annu. Rev. Biochem.* **2010**, *79*, 1.

[11] a) K. M. Ryan, G. D. Birnier, *Biochem. J.* **1996**, *314*, 713; b) V. H. Cowling, M. D. Cole, *Semin. Cancer Biol.* **2006**, *16*, 242.

[12] a) R. Gurlie, T. H. Duong, K. Zakrzewska, *Biopolymers* **1999**, *49*, 313; b) R. L. Winston, J. M. Gottesfeld, *Chem. Biol.* **2000**, *7*, 245; c) S. K. Nair, S. K. Burley, *Cell* **2003**, *112*, 193; d) L. Ma, Y. Y. Sham, K. J. Walters, H. C. Towle, *Nucleic Acids Res.* **2007**, *35*, 35.

[13] E. C. Turner, C. H. Cureton, C. J. Weston, O. S. Smart, R. K. Alleman, *Chem. Biol.* **2004**, *11*, 69.

[14] L. Guerrero, O. S. Smart, C. J. Weston, D. C. Burns, G. A. Woolley, R. K. Allemann, *Angew. Chem.* **2005**, *117*, 7956; *Angew. Chem. Int. Ed.* **2005**, *44*, 7778.

[15] Interestingly, studies focusing on the leucine zipper region of b-HLH-ZIP proteins further indicate the inferior stability of their dimerizing interfaces, in contrast to the bZIP counterparts Jun, Fos, and GCN4: C. Muhle-Goss, T. Gibson, P. Schuck, D. Schubert, D. Nalis, M. Nilges, A. Pastore, *Biochemistry* **1994**, *33*, 11296.

[16] In this respect, the heterodimeric Jun-Fos bZIP oncoprotein bears special mentioning, combining cMyc-like cancer relevance with GCN4-like structural tractability.

[17] D. Verzele, L. L. G. Carrette, A. Madder, *Drug Discovery Today Technol.* **2010**, *7*, e115.

[18] Employing peptide/protein assemblies as promising alternatives for small-molecule approaches acting on the DNA–protein interface (complementing the aforementioned protein–protein disruptors), the superior control of recognition specificity (cited above) has already led to success stories with minor groove binding Dervan polyamides and major groove targeting zinc finger proteins (further stimulated by their design modularity, synthetic accessibility, and uptake potential). Further reading: a) T. C. Uil, H. J. Haisma, M. G. Rots, *Nucleic Acids Res.* **2003**, *31*, 6064; b) A. C. Jamieson, J. C. Miller, C. O. Pabo, *Nat. Rev. Drug Discovery* **2003**, *2*, 361; c) P. D. Blancafort, J. Segal, C. F. Barbas III, *Mol. Pharmacol.* **2004**, *66*, 1361; d) K. Schmitz, U. Schepers, *Angew. Chem.* **2004**, *116*, 2526; *Angew. Chem. Int. Ed.* **2004**, *43*, 2472; e) J. T. Koh, J. Zheng, *ACS Chem. Biol.* **2007**, *2*, 599; f) X. Cai, P. J. Gray Jr., D. D. Von Hoff, *Cancer Treat. Rev.* **2009**, *35*, 437; g) C. Li, C. Du, H. Tian, C. Jiang, M. Du, Y. Liu, R.-Z. Qiao, Y.-X. Jia, Y.-F. Zhao, *Chem. Eur. J.* **2010**, *16*, 12935.

[19] a) C. O. Pabo, R. T. Sauer, *Annu. Rev. Biochem.* **1992**, *61*, 1053; b) I. Ghosh, S. Yao, J. Chmielewski, *Comprehensive Natural Products Chemistry* (Eds.: D. Barton, K. Nakanishi), Pergamon, Oxford, **1999**, chap. 7.13, p. 477; c) C. W. Garvie, C. Wolberger, *Mol. Cell* **2001**, *8*, 937.

[20] a) H. C. Hurst, *Protein Profile* **1994**, *1*, 123; b) T. Ellenberger, *Curr. Opin. Struct. Biol.* **1994**, *4*, 12; c) S. K. Nair, S. K. Burley, *Curr. Top. Microbiol. Immunol.* **2006**, *302*, 123.

[21] T. E. Ellenberger, C. J. Brandl, K. Struhl, S. C. Harrison, *Cell* **1992**, *71*, 1223.

[22] a) L. Jen-Jacobsen, L. E. Engler, L. A. Jacobsen, *Structure* **2000**, *8*, 1015; b) P. L. Privalov, A. I. Dragan, C. Crane-Robinson, K. J. Breslauer, D. P. Remeta, C. A. S. A. Minetti, *J. Mol. Biol.* **2007**, *365*, 1.

[23] Reviewed in: a) S. Sato, M. Hagihara, K. Sugimoto, T. Morii, *Chem. Eur. J.* **2002**, *8*, 5066; b) M. E. Vázquez, A. M. Caamaño, J. L. Mascareñas, *Chem. Soc. Rev.* **2003**, *32*, 338; c) E. Pazos, J. Mosquera, M. E. Vázquez, J. L. Mascareñas, *ChemBioChem* **2011**, *12*, 1958.

[24] Selected reading: a) N. Jones, *Cell* **1990**, *61*, 9; b) R. Fairman, R. K. Beran-Steed, S. J. Anthony-Cahill, J. D. Lear, W. F. Stafford III, W. F. DeGrado, P. A. Benfield, S. L. Brenner, *Proc. Natl. Acad. Sci. USA* **1993**, *90*, 10429; c) C. Park, J. L. Campbell, W. A. Goddard III, *J. Am. Chem. Soc.* **1996**, *118*, 4235; d) S. J. Metallo, A. Schepartz, *Nat. Struct. Mol. Biol.* **1997**, *4*, 115; e) S. Sauvé, J.-F. Naud, P. Lavigne, *J. Mol. Biol.* **2007**, *365*, 1163; f) O. Ecevit, M. A. Khan, D. J. Goss, *Biochemistry* **2010**, *49*, 2627.

[25] Recent examples: a) E. K. Liebler, U. Diederichsen, *Org. Lett.* **2004**, *6*, 2893; b) M. Zhou, I. Ghosh, *Org. Lett.* **2004**, *6*, 3561; c) A. C. Beltran, P. E. Dawson, J. M. Gottesfeld, *ChemBioChem* **2005**, *6*, 104; d) J. Svobodová, C. Cabrele, *ChemBioChem* **2006**, *7*, 1164; e) O. Vázquez, M. E. Vázquez, J. B. Blanco, L. Castedo, J. L. Mascareñas, *Angew. Chem.* **2007**, *119*, 7010; *Angew. Chem. Int. Ed.* **2007**, *46*, 6886; f) O. Vázquez, J. B. Blanco-Canosa, E. M. Vázquez, J. Martínez-Costas, L. Castedo, J. L. Mascareñas, *ChemBioChem* **2008**, *9*, 2822; g) J. Xu, G. Chen, A. T. De Jong, S. H. Shahravan, J. A. Shin, *J. Am. Chem. Soc.* **2009**, *131*, 7839; h) Y. Azuma, M. Imanishi, T. Yoshimura, T. Kawabata, S. Futaki, *Angew. Chem.* **2009**, *121*, 6985; *Angew. Chem. Int. Ed.* **2009**, *48*, 6853; i) S. Pensato, M. Renda, F. Leccia, M. Saviano, L. D. D'Andrea, C. Pedone, P. V. Pedone, A. Romanelli, *Biopolymers* **2010**, *93*, 434; j) R. S. Tu, R. Marullo, R. Pynn, R. Bitton, H. Bianco-Peled, M. V. Tirrell, *Soft Matter* **2010**, *6*, 1035.

[26] Minimalist strategy: as an alternative to dimerization approaches, the net unfavorable binding free energy of the downsizing process is compensated by preorganization (Ala-substitution, "stapling", avian pancreatic polypeptide grafting) or conjugation to an accessory module (Dervan peptide, intercalator) assisting in DNA binding. Further reading in addition to ref.[13,14,23b,23c,25e–25g], focusing on Myc: a) D. E. Fisher, L. A. Parent, P. A. Sharp, *Cell* **1993**, *72*, 467; b) C. Takemoto, D. E. Fisher, *Gene Expression* **1995**, *4*, 311.

[27] R. V. Talanian, C. J. McKnight, P. S. Kim, *Science* **1990**, *249*, 769.

[28] Further used by Goddard III et al. with the homodimeric Jun bZIP: C. Park, J. L. Campbell, W. A. Goddard III, *Proc. Natl. Acad. Sci. USA* **1993**, *90*, 4892.

[29] M. Pellegrini, R. H. Ebright, *J. Am. Chem. Soc.* **1996**, *118*, 5831.

[30] Selected examples: a) B. Cuenoud, A. Schepartz, *Science* **1993**, *259*, 510; b) C. R. Palmer, L. S. Sloan, J. C. Adrian Jr., B. Cuenoud, D. N. Paolella, A. Schepartz, *J. Am. Chem. Soc.* **1995**, *117*, 8899.

[31] Further examples (in addition to ref.[7,23a]): a) Y. Aizawa, Y. Sugiura, T. Morii, *Biochemistry* **1999**, *38*, 1626; b) A. Hirata, M. Ueno, Y. Aizawa, K. Ohkubo, T. Morii, S. Yoshikawa, *Bioorg. Med. Chem.* **2005**, *13*, 3107.

[32] A. M. Caamaño, M. E. Vázquez, J. Martínez-Costas, L. Castedo, J. L. Mascareñas, *Angew. Chem.* **2000**, *112*, 3234; *Angew. Chem. Int. Ed.* **2000**, *39*, 3104.

[33] Selected reviews: a) P. Wallimann, T. Marti, A. Furer, F. Diederich, *Chem. Rev.* **1997**, *97*, 1567; b) A. Enhsen, W. Kramer, G. Wess, *Drug Discovery Today* **1998**, *3*, 409; c) R. Maltais, M. R. Tremblay, L. C. Ciobanu, D. Poirier, *J. Comb. Chem.* **2004**, *6*, 443; d) E. Virtanen, E. Kolehmainen, *Eur. J. Org. Chem.* **2004**, 3385; e) D. B. Salunke, B. G. Hazra, V. S. Pore, *Curr. Med. Chem.* **2006**, *13*, 813; f) A. P. Davis, *Molecules* **2007**, *12*, 2106; g) Nonappa, U. Maitra, *Org. Biomol. Chem.* **2008**, *6*, 657.

[34] a) R. Boyce, G. Li, H. P. Nestler, T. Suenaga, W. C. Still, *J. Am. Chem. Soc.* **1994**, *116*, 7955; b) Y. Chen, T. Suenaga, W. C. Still, *J. Am. Chem. Soc.* **1996**, *118*, 1813.

[35] Recent examples from our group, in addition to further precedents in above reviews (ref.[33]): a) C. A. Bodé, T. Bechet, E. Prodhomme, K. Gheysen, P. Gregoir, J. C. Martins, C. P. Muller, A. Madder, *Org. Biomol. Chem.* **2009**, *7*, 3391; b) Figaroli, S. A. Madder, *Tetrahedron* **2010**, *66*, 6912.
[36] W. Kramer, *Biol. Chem.* **2011**, *392*, 77.
[37] L. J. D'Souza, U. Maitra, *J. Org. Chem.* **1996**, *61*, 9494.
[38] H. Li, L. Wang, *Org. Biomol. Chem.* **2003**, *1*, 3507.
[39] a) S. Yang, S. S. Cho, Y. Levy, M. S. Cheung, H. Levine, P. G. Wolynes, J. N. Onuchic, *Proc. Natl. Acad. Sci. USA* **2004**, *101*, 13786; b) W. K. Meisner, T. R. Sosnick, *Proc. Natl. Acad. Sci. USA* **2004**, *101*, 13478; c) T. Kameda, S. Takada, *Proc. Natl. Acad. Sci. USA* **2006**, *103*, 17765; d) J. Garner, M. M. Hardling, *Org. Biomol. Chem.* **2007**, *5*, 3577.
[40] D. Verzele, A. Madder, *Eur. J. Org. Chem.* **2007**, *11*, 1793.
[41] D. Verzele, J. L. Goeman, A. Madder, *ARKIVOC* **2007**, *x*, 325 (commemorative issue in honor of Prof. Dr. A. Krief).
[42] I. Coin, M. Beyermann, M. Bienert, *Nat. Protoc.* **2007**, *2*, 3247.
[43] Remarkably, although (obviously) recommending their novel native chemical ligation alternative, Kent et al. demonstrate identical peptide integrity and constitution with a simple, linear SPPS approach in following example: W. Lu, M. A. Quasim, S. B. H. Kent, *J. Am. Chem. Soc.* **1996**, *118*, 8518.
[44] C. P. Holmes, D. G. Jones, *J. Org. Chem.* **1995**, *60*, 2318.
[45] C. P. Holmes, *J. Org. Chem.* **1997**, *62*, 2370.
[46] It is noted that compound numbers are used interchangeably between solid-supported molecules and liberated counterparts.
[47] F. Gaggini, A. Porcheddu, G. Reginato, M. Rodriquez, M. Taddei, *J. Comb. Chem.* **2004**, *6*, 805.
[48] a) A. Madder, N. Farcy, N. G. C. Hosten, H. De Muynck, P. J. De Clercq, J. Barry, A. P. Davis, *Eur. J. Org. Chem.* **1999**, 2787; b) L. L. G. Carrette, D. Verzele, A. Madder, *Tetrahedron Lett.* **2010**, *51*, 2106.
[49] G. Talbo, J. D. Wade, N. Dawson, M. Manoussios, G. W. Tregear, *Lett. Pept. Sci.* **1997**, *4*, 121.
[50] A. M. Schaiberger, J. A. Moss, *J. Am. Soc. Mass Spectrom.* **2008**, *19*, 614.
[51] R. V. Talanian, J. McKnight, R. Rutkowski, P. S. Kim, *Biochemistry* **1992**, *31*, 6871.
[52] All chiral α-amino acids used in this paper possessed the L-configuration. Throughout this work, N^{α}-Fmoc-protected residues with standard acid-sensitive side chain PGs were used: Asp(O*t*Bu) [D], Glu(O*t*Bu) [E], His(Trt) [H], Lys(Boc) [K], Asn(Trt) [N], Gln(Trt) [Q], Arg(Pbf) [R], Ser(*t*Bu) [S], Thr(*t*Bu) [T].
[53] C. K. Taylor, P. W. Abel, M. Hulce, D. D. Smith, *J. Pept. Res.* **2005**, *65*, 84.
[54] Hindrance of the DIPEA base provides prolonged (>3 h) stability of the N^{α}-Fmoc protectant: C. D. Chang, M. Waki, M. Ahmed, J. Meienhofer, E. O. Lundell, J. D. Haug, *Int. J. Pept. Protein Res.* **1980**, *15*, 59.
[55] Efficient couplings indeed critically depend on concentration of activated species, and a 0.15 M concentration is recommended in: G. A. Grant (Ed.), *Synthetic Peptides, A User's Guide*, W. H. Freeman and Company, New York, **1992**, p. 124.
[56] The detrimental effect of erroneous resin irradiation (prolonged and/or insufficiently immersed) is worth mentioning, resulting in decomposition of compounds.
[57] Opaque UV-cleaved solutions have additionally been noticed.
[58] Further details can be found in the Experimental Section. In brief, gradient 1 refers to a 0 to 100% linear increase of B (vs. A) over 15 min [A = H_2O + TFA (0.1%), B = ACN; flow = 1.0 mL min^{-1}]. Pre- and postflushing is included in the chromatographic output.
[59] Desirable given the metabolic lability of cMyc ($t_{1/2}$ = 20–30 min).
[60] Recent example thereof (in addition to the aforementioned ones on bile acids specifically): P. Ingallinella, E. Bianchi, N. A. Ladwa, Y. Wang, R. Hrin, M. Veneziano, F. Bonelli, T. J. Ketas, J. P. Moore, M. D. Miller, A. Pessi, *Proc. Natl. Acad. Sci. USA* **2009**, *106*, 5801.
[61] These combinations bear similarities to precedents by Morii et al. (cited earlier), in which the cMyc-cMyc association resembles the inherently weak MyoD-MyoD model (ref.[7]), whereas the unnatural union between the bZIP GCN4 and b-HLH-ZIP cMyc/Max strands parallels the GCN4-EMBP1 bZIP-bZIP heterodimer (ref.[31b]).
[62] a) O. Dangles, F. Guibé, G. Balavoine, S. Lavielle, A. Marquet, *J. Org. Chem.* **1987**, *52*, 4984; b) F. Guibé, *Tetrahedron* **1998**, *54*, 2967.
[63] a) S. L. Cohen, B. T. Chait, *Anal. Chem.* **1996**, *68*, 31; b) K. B. Green-Church, P. A. Limbach, *Anal. Chem.* **1998**, *70*, 5322; c) G. H. Bird, A. R. Lajmi, J. A. Shin, *Anal. Chem.* **2002**, *74*, 219; d) A. J. Hoteling, W. J. Erb, R. J. Tyson, K. G. Owens, *Anal. Chem.* **2004**, *76*, 5157.
[64] a) As mentioned in: S. Peluso, P. Dumy, C. Nkubana, Y. Yokokawa, M. Mutter *J. Org. Chem.* **1999**, *46*, 7114; b) B. D. Larsen, A. Holm, *Int. J. Pept. Protein Res.* **1994**, *43*, 1; c) J. P. Tam, Y. Lu, *J. Am. Chem. Soc.* **1995**, *117*, 12058.
[65] M. Rinnová, M. Nováková, V. Kašička, J. Jiráček, *J. Pept. Sci.* **2000**, *6*, 355.
[66] S. M. Sternson, S. L. Schreiber, *Tetrahedron Lett.* **1998**, *39*, 7451.
[67] Which proved to be an important step to obtain satisfying flocculation upon Et_2O trituration, as further mentioned in: Merck Novabiochem Catalog **2008/2009**. Synthesis Notes, p. 3.30.
[68] Intense signals for PG species could significantly be reduced by thorough sonication of the precipitated material in Et_2O. Because these peaks exhibit UV activity, they are most probably explained by debris of the Pbf and Trt groups. The latter one (the cation) might be irreversibly converted into triphenylmethane by the potent TIS scavenger. Merck Novabiochem Catalog **2008/2009**. Synthesis Notes, p. 3.32.
[69] Corroborated by Merck Novabiochem Catalog **2006/2007**. Synthesis Notes, p. 2.54.
[70] Protocol adapted from: B. A. Bunin, *The Combinatorial Index*, Academic Press, London, UK, **1998**.

Received: September 17, 2012
Published Online: December 6, 2012